

UNCLASSIFIED

AD NUMBER	
AD385450	
CLASSIFICATION CHANGES	
TO:	UNCLASSIFIED
FROM:	SECRET
LIMITATION CHANGES	
TO: Approved for public release; distribution is unlimited.	
FROM: Distribution authorized to U.S. Gov't. agencies only; Test and Evaluation; NOV 1967. Other requests shall be referred to Aeronautical Systems Div., Wright-Patterson AFB, OH 45433.	
AUTHORITY	
ASD ltr 28 Nov 1972 ; ASD ltr 16 Aug 1977	

THIS PAGE IS UNCLASSIFIED

DECLASSIFIED / UNCLASSIFIED

AEDC-TR-67-252

ARO, INC.
DOCUMENT CONTROL

NO **IG-681-343**

COPY 1 OF 41

SERIES A **PAGES** 46

300 444



WIND TUNNEL INVESTIGATION OF A 1/8-SCALE AMSA AIRCRAFT-INLET MODEL AT TRANSONIC AND SUPERSONIC MACH NUMBERS (U)

JAN 29 1968

JUN 4 1968

44-38861-1000 JUN 18 1969

AIR FORCE
RYUN 1970

JUN 23 1971

JUL 28 1972

Lawrence L. Galigher

ARO, Inc. PROPERTY OF U. S. AIR FORCE
AEDC LIBRARY JUN 1970
AF 40(600)1200

November 1967

CLASSIFICATION CANCELLED CHANGED TO
BY UT OR Y , *No lead memo #917, 1 Dec*
8 Dec 7

NOTE :
PUB RELEASE,
UNLIMITED

**PROPULSION WIND TUNNEL FACILITY
ARNOLD ENGINEERING DEVELOPMENT CENTER
AIR FORCE SYSTEMS COMMAND**

ARNOLD AIR FORCE STATION, TENNESSEE

DECLASSIFIED / UNCLASSIFIED

PROPERTY OF U. S. AIR FORCE
AF 40(600)1200

GROUP 3
Downgraded at 12 year intervals;
Not automatically declassified.
DOD DIR 5200 10

AEDC TECHNICAL LIBRARY



5 0720 00031 6325

NOTICES

When U. S. Government drawings specifications, or other data are used for any purpose other than a definitely related Government procurement operation, the Government thereby incurs no responsibility nor any obligation whatsoever, and the fact that the Government may have formulated, furnished, or in any way supplied the said drawings, specifications, or other data, is not to be regarded by implication or otherwise, or in any manner licensing the holder or any other person or corporation, or conveying any rights or permission to manufacture, use, or sell any patented invention that may in any way be related thereto.

Qualified users may obtain copies of this report from the Defense Documentation Center.

References to named commercial products in this report are not to be considered in any sense as an endorsement of the product by the United States Air Force or the Government.

Do not return this copy. When not needed, destroy in accordance with pertinent security regulations.

DECLASSIFIED / UNCLASSIFIED

**WIND TUNNEL INVESTIGATION OF A 1/8-SCALE
AMSA AIRCRAFT-INLET MODEL AT
TRANSONIC AND SUPERSONIC MACH NUMBERS (U)**

Lawrence L. Galigher
ARO, Inc.

In addition to security requirements which be met, this document is subject to export controls and each transmission to foreign governments or foreign nations may be made only with prior approval of ASD (ASZD), Wright-Patterson AFB, Ohio.

In addition to security requirements which be met, this document and must be transmitted outside the Department of Defense must have prior approval of ASD (ASZD), Wright-Patterson AFB, Ohio.

This material contains information affecting the national defense of the United States within the meaning of the Espionage Laws (Title 18, U.S.C., sections 793 and 794) the transmission or revelation of which in any manner to an unauthorized person is prohibited by law.

Distribution limited to U. S. Gov't. Agencies only; Test and evaluation; No other requests for this document must be referred to Commander, Aeronautical Systems Div., AFHQ: YHT, Wright-Patterson AFB, Ohio 45433. Per T.O. 2, 15 January, 1973

CLASSIFICATION CANCELLED (CONTINUED TO 1)
BY 001-02 X J. H. H. H. Memo # 812, 1 Dec 72
BY *E. C. H. H.*
Name and Position of Individual
Date 8 Dec 72

UNCLASSIFIED
This page is Unclassified

DECLASSIFIED / UNCLASSIFIED

DECLASSIFIED / UNCLASSIFIED**FOREWORD**

(U) The work reported herein was done at the request of the Aeronautical Systems Division (ASD), Air Force Systems Command (AFSC), for the General Dynamics Corporation, Fort Worth, Texas, under Program Element 6340683F, Program Area 139A.

(U) The results of tests presented were obtained by ARO, Inc. (a subsidiary of Sverdrup & Parcel and Associates, Inc.), contract operator of the Arnold Engineering Development Center (AEDC), AFSC, Arnold Air Force Station, Tennessee, under Contract AF40(600)-1200. The test was conducted from August 7 through September 9, 1967, under ARO Project No. PT0741, and the manuscript was submitted for publication on October 27, 1967.

(U) This report contains no classified information extracted from other classified documents.

(U) This technical report has been reviewed and is approved.

Richard W. Bradley
Lt Col, USAF
AF Representative, PWT
Directorate of Test

Leonard T. Glaser
Colonel, USAF
Director of Test

DECLASSIFIED / UNCLASSIFIED

ii

SECRET
This page is Unclassified

UNCLASSIFIED ABSTRACT

(U) Test results are presented for a 1/8-scale inlet model of a proposed AMSA air induction system at transonic and supersonic Mach numbers. The effects of spike bleed pattern and inlet orientation are presented. Compressor face total-pressure recovery and flow distortion data are presented as a function of spike position, compressor-face mass-flow ratio, spike boundary-layer bleed mass-flow ratio, angle of attack, angle of sideslip, and free-stream Mach number.

This document is subject to special export controls and each transmittal to foreign countries or foreign nationals must be made only with prior approval of ASD, CAZ, Wright-Patterson AFB, Ohio.

Distribution limited to U. S. Gov't agencies only; Test and Evaluation only. Other requests for this document must be referred to Commander, Aeronautical Systems Div., Attn: [redacted] Wright-Patterson AFB, Ohio 45433. Per TAB 73-2, 15 January, 1973.

DECLASSIFIED / UNCLASSIFIED CONTENTS

	<u>Page</u>
ABSTRACT.	iii
NOMENCLATURE.	vii
I. INTRODUCTION	1
II. APPARATUS	
2.1 Test Facilities	1
2.2 Test Article	2
2.3 Instrumentation.	3
III. PROCEDURE.	
3.1 General	3
3.2 Accuracy of Measurements	4
IV. RESULTS AND DISCUSSION	
4.1 Isolated Inlet Tests	5
4.2 Inlet-Airplane Tests	6
V. CONCLUSIONS	8

APPENDIXES

I. ILLUSTRATIONS

Figure

1. Location of AMSA 1/8-Scale Inlet Model in Tunnel 16T and Tunnel 16S Test Sections	11
2. Sketch of AMSA 1/8-Scale Inlet Model	12
3. Sketch of the Proposed AMSA	13
4. Inlet Airplane Model Installation in Test Section	
a. Tunnel 16T	14
b. Tunnel 16S	15
5. Isolated Inlet Installation in Test Section	
a. Single Inlet	16
b. Dual Inlets: Nonstaggered Arrangement	17
c. Dual Inlets: Staggered Arrangement	18
6. Dimensioned Sketch of Model Nacelle.	19
7. Spike Boundary-Layer Bleed Pattern	20
8. Inlet Spike Contours	21

DECLASSIFIED / UNCLASSIFIED

Figure	Page
9. Compressor-Face Station Instrumentation.	22
10. (S) Effect of Spike Bleed Flow on Inlet Performance; I_1^{27} Spike, $M_\infty = 2.06$, $\alpha = 0$ deg, $\beta = 0$ deg, $X/R = 1.59$, $W\sqrt{\theta/\delta_2} = 185 \text{ lb}_m/\text{sec}$	23
11. (S) Effect of Spike Position on Inlet Performance; I_1^{27} Spike, $M_\infty = 2.06$, $\alpha = 0$ deg, $\beta = 0$ deg, $W\sqrt{\theta/\delta_2} = 180 \text{ lb}_m/\text{sec}$	24
12. (S) Effect of Spike Bleed Pattern on Inlet Performance; I_1^{27} Spike, $M_\infty = 2.06$, $\alpha = 0$ deg, $\beta = 0$ deg, $X/R = 1.63$	25
13. (S) Mutual Interference Effects of Nonstaggered, Dual-Inlet Orientation on Inlet Performance; I_1^{27} Spike, $M_\infty = 2.06$, $\alpha = 0$ deg, $\beta = 0$ deg, $X/R = 1.63$	26
14. (S) Mutual Interference Effect of Staggered Dual-Inlet Orientation on Inlet Performance; I_1^{27} Spike, $M_\infty = 2.06$, $\alpha = 0$ deg, $\beta = 0$ deg, $(X/R)_{\text{Inb'd}} = 1.63$, $(X/R)_{\text{Outb'd}} = 1.67$	27
15. (S) (U) Effect of Spike Position on Inlet Performance; $\alpha = 5$ deg, $\beta = 0$ deg a. (S) $M_\infty = 0.85$, $W\sqrt{\theta/\delta_2} = 260 \text{ lb}_m/\text{sec}$ b. (S) $M_\infty = 1.20$, $W\sqrt{\theta/\delta_2} = 260 \text{ lb}_m/\text{sec}$ c. (S) $M_\infty = 1.75$, $W\sqrt{\theta/\delta_2} = 220 \text{ lb}_m/\text{sec}$ d. (S) $M_\infty = 2.05$, $W\sqrt{\theta/\delta_2} = 196 \text{ lb}_m/\text{sec}$ e. (S) $M_\infty = 2.20$, $W\sqrt{\theta/\delta_2} = 180 \text{ lb}_m/\text{sec}$	28 29 30 31 32
16. (S) Effect of Spike Bleed Flow on Inlet Performance; I_1^{27} Spike, $M_\infty = 2.20$, $\alpha = +5$ deg, $\beta = 0$ deg, $W\sqrt{\theta/\delta_2} = 180 \text{ lb}_m/\text{sec}$	33
17. Effect of Angle of Attack on Inlet Performance; $\beta = 0$ deg.	34
18. Effect of Angle of Sideslip on Inlet Performance; $\alpha = 6.2$ deg.	35
19. Optimum Inlet Performance; $\alpha = +5$ deg, $\beta = 0$ deg . . .	36

DECLASSIFIED / UNCLASSIFIED

II. TABLE

I. Accuracy of Measurements.	37
--------------------------------------	----

NOMENCLATURE

BL	Buttock line
D_2	Compressor-face total-pressure distortion, $\left[(p_{t2})_{\max} - (p_{t2})_{\min} \right] / (p_{t2})_{\text{avg}}$
I_1	Inlet spike with 15-deg first-cone half-angle
M	Mach number
m_2/m_1	Ratio of compressor-face station mass flow to inlet capture mass flow. The inlet capture mass flow is defined as the mass flow passing through an area equivalent to the cowl area when projected on a plane normal to the spike centerline
m_{sb}/m_1	Ratio of spike bleed mass flow to inlet capture mass flow
N_2	Compressor-face total-pressure recovery, $(p_{t2})_{\text{avg}} / p_{t\infty}$
p_t	Total pressure, psfa
R	Inlet cowl radius at cowl leading edge
T_t	Total temperature, °R
WL	Waterline
w	Simulated full-scale weight flow at compressor-face station, lb _m /sec
X	Distance from cowl leading edge to spike tip, in.
α	Angle of attack of model wing chord line, deg
β	Angle of sideslip, positive nose left, deg
δ_2	Ratio of compressor-face average total pressure to standard sea-level pressure, $(p_{t2})_{\text{avg}}/2116$

SYMBOLS, ABBREVIATIONS, AND DEFINITIONS

θ Ratio of free-stream total temperature to standard sea-level temperature, $T_{t\infty}/519$

SUBSCRIPTS

1	Inlet lip station
2	Compressor-face station
avg	Average
Inb'd	Inboard inlet
max	Maximum
min	Minimum
Outb'd	Outboard inlet
∞	Free-stream conditions

SUPERSSCRIPTS

10, 15, 20, 24, and 27	Inlet spike second-cone deflection angle, deg
---------------------------	---

~~SECRET~~

DECLASSIFIED / UNCLASSIFIED

**SECTION I
INTRODUCTION**

(U) Tests were conducted in the Propulsion Wind Tunnel, Transonic (16T) and Supersonic (16S) to determine inlet performance characteristics of a 1/8-scale, partial span model of the Advanced Manned Strategic Aircraft (AMSA) as proposed by the General Dynamics Corporation, Fort Worth Division.

(S) The objectives of the tests were to evaluate some spike and cowl design variations and nacelle position effects (spacing and stagger) from both the isolated inlet and inlet-airplane standpoint.

(S) This report is concerned with the significant test results obtained for the basic cowl configuration at free-stream Mach numbers from 0.85 to 2.20. The complete test data were forwarded to the test user and are available at AEDC.

**SECTION II
APPARATUS**

2.1 TEST FACILITIES

(U) Tunnel 16T is a closed-circuit, continuous flow wind tunnel capable of operating at Mach numbers from 0.55 to 1.60. The tunnel can be operated over a stagnation pressure range from approximately 160 to 4000 psfa and over a stagnation temperature range from 80 to 160°F. The tunnel specific humidity is controlled by removing tunnel air and supplying conditioned makeup air from an atmospheric dryer. Perforated walls in the test section allow continuous operation through the Mach number range with a minimum of wall interference.

(U) Tunnel 16S is a closed-circuit, continuous flow wind tunnel that currently can be operated at Mach numbers from 1.65 to 3.10. The tunnel can be operated over a stagnation pressure range from approximately 100 to 1800 psfa and over a stagnation temperature range from 150 to 435°F. The tunnel specific humidity is controlled by removing tunnel air and supplying conditioned makeup air from an atmospheric dryer.

~~SECRET~~

DECLASSIFIED / UNCLASSIFIED

DECLASSIFIED / UNCLASSIFIED

(U) A more extensive description of each tunnel and its operating characteristics is contained in the Test Facilities Handbook.¹ A dimensioned sketch showing the model location and the sting support arrangement in both the Tunnel 16T and Tunnel 16S test sections is presented in Fig. 1 (Appendix I).

2.2 TEST ARTICLE

2.2.1 Wing-Fuselage Configuration

(S) The model is a 1/8-scale general configuration of the basic AMSA airplane with the variable swept wings in the fully retracted position. The wing tips, aft of the outboard inlet, cowl lip station, and horizontal stabilizer were removed to reduce aerodynamic loads on the wind tunnel model. Dimensioned sketches of the model and the proposed full-scale AMSA are shown in Figs. 2 and 3, respectively. Photographs of the model installation in Tunnel 16T and Tunnel 16S are presented in Fig. 4.

2.2.2 Inlet Configuration

(S) The air induction system for the proposed AMSA, as shown previously in Fig. 3, consists of four external compression, axisymmetric double-cone inlets located beneath the wings and attached to the fuselage in dual-inlet arrangement. Only the dual-inlet arrangement for the left side of the fuselage was installed on the model for the inlet-airplane phase of testing. During the isolated inlet phase of testing, a mounting bracket was used to position both a single-inlet installation and a dual-inlet installation ahead of the sting. For the dual-inlet installation, separation distances of 0.70, 0.84, and 1.00 inlet diameters were investigated for a nonstaggered arrangement, and a separation distance of 0.84 inlet diameters was investigated for a staggered arrangement. In the staggered arrangement the outboard inlet was located 3.5 inlet diameters downstream of the inboard inlet. Photographs of the isolated single-inlet installation and the isolated dual-inlet installation in both the nonstaggered and staggered arrangements are shown in Fig. 5.

¹Test Facilities Handbook (6th Edition). "Propulsion Wind Tunnel Facility, Vol. 5." Arnold Engineering Development Center, November 1966.

DECLASSIFIED / UNCLASSIFIED

(S) The inlets had 9.5-deg cowl lip angles and inlet capture areas of 14.875 in.². They were geometrically similar, both internally and externally, to full-scale inlets from the cowl lip to the compressor-face station (nacelle station 14.375). Compressor-face airflow control was obtained with a variable position plug valve downstream of the compressor face. A sketch of the model nacelle, including tables of the cowl internal and external contours, is shown in Fig. 6.

(S) Five interchangeable double-cone inlet spikes were provided for each inlet. The spikes had a 15-deg first-cone half angle with second-cone deflection angles of 10, 15, 20, 24, and 27 deg. They were remotely translatable and, with the exception of the two spikes having second-cone deflection angles of 10 and 15 deg, had boundary-layer bleed holes on the second-cone surface. Spike boundary-layer bleed pattern variations were accomplished by opening selected rows of bleed holes that were initially closed with a filling compound prior to testing. Spike bleed flow was ducted internally through the spike centerbody and vented overboard. Spike bleed control was obtained with a variable position plug valve located within the inlet actuator housing. The two bleed patterns investigated during this test are shown in Fig. 7. A sketch of the spike, including tables of the spike contours, is shown in Fig. 8.

2.3 INSTRUMENTATION

(U) Inlet performance in terms of total-pressure recovery and flow distortion were obtained from compressor-face total-pressure measurements; the orifice locations are shown in Fig. 9. A dynamic transducer was mounted in the duct wall at the compressor face of each inlet to monitor inlet stability. Spike boundary-layer bleed and compressor-face mass flows were measured using calibrated metering plugs in conjunction with static and total-pressure measurements and free-stream total temperature measurements.

(U) Linear potentiometers were used to measure spike position, spike bleed plug position, and compressor-face flow plug position.

SECTION III PROCEDURE

3.1 GENERAL

(S) The AMSA model was tested in Tunnel 16T at nominal free-stream Mach numbers of 0.85 and 1.20. Free-stream total temperature was maintained at 120°F, and free-stream total pressure was

~~SECRET~~
DECLASSIFIED / UNCLASSIFIED

maintained at 1560 and 1200 psfa at Mach numbers 0.85 and 1.20 respectively. In Tunnel 16S the model was tested at Mach numbers from 1.75 to 2.20. Free-stream total temperature and total pressure were maintained at 200°F and 1100 psfa, respectively, through the Mach number range. The model angle of attack and angle of sideslip were varied from 0 to +14 deg and from -8 to +8 deg, respectively. The majority of the data taken with the model in a yawed attitude was taken at a nominal 6.2-deg angle of attack.

(S) After tunnel free-stream total pressure and Mach number were established, the model was positioned to the desired angle of attack and/or angle of sideslip. Steady-state pressure measurements were obtained by setting the desired spike position and spike bleed flow and setting selected compressor-face corrected weight flow by varying the primary duct plug position. Except when determining the influence of spike bleed flow rate on inlet performance, the spike bleed flow was gradually increased until further increases in the spike bleed flow had no effect on inlet recovery. Inlet stability was determined by monitoring the output of the dynamic pressure transducer mounted near the compressor face. The initial indication of pressure fluctuation at the compressor-face station defined the inlet stability limit as presented in this report.

3.2 ACCURACY OF MEASUREMENTS

(U) The probable errors associated with the various tunnel and model parameters are listed in Table I (Appendix II). Since the data presented in this report were obtained from single sample measurements, the errors listed in Table I are the estimated uncertainties of the data based upon the accuracy of the instrumentation components and tunnel calibration data.

SECTION IV RESULTS AND DISCUSSION

(S) Inlet performance in terms of compressor-face total-pressure recovery and flow distortion is presented as a function of spike position, compressor-face mass-flow ratio, spike boundary-layer bleed mass-flow ratio, angle of attack, angle of sideslip, and free-stream Mach number.

DECLASSIFIED / UNCLASSIFIED

~~SECRET~~
DECLASSIFIED / UNCLASSIFIED

(6) The predicted cruise attitude of the AMSA model, as discussed in this report, is assumed to be +5 deg angle of attack and 0 deg angle of sideslip through the Mach number range from 0.85 to 2.20. The total-pressure recovery and flow-distortion data presented for the inlet-airplane phase of testing are those values that were obtained for nominal compressor-face corrected airflows of 260, 260, 220, 196, and 180 lb_m/sec at Mach numbers of 0.85, 1.20, 1.75, 2.05, and 2.20, respectively. During the isolated inlet phase of testing, the majority of data was obtained for a nominal compressor-face corrected airflow of 180 lb_m/sec and at Mach number 2.06, which was estimated as the local Mach number in the inlet flow field generated by the wing-fuselage combination at free-stream Mach number 2.20.

4.1 ISOLATED INLET TESTS

4.1.1 Spike Bleed Flow

(8) The effect of spike boundary-layer bleed flow on inlet performance at Mach number 2.06 is presented in Figs. 10 through 12. The two spike bleed patterns investigated (bleed patterns 5 and 6) provided the same improvement in total-pressure recovery. As shown in Fig. 10, recovery increased and distortion remained essentially unchanged as spike bleed flow was increased to the maximum obtainable value. At the optimum spike position of $X/R = 1.63$, as determined from Fig. 11, maximum spike bleed flow increased maximum recovery approximately 1 percent for a nominal corrected airflow of 180 lb_m/sec. The data presented in Fig. 11 also show that spike position at maximum recovery was less critical with spike bleed flow than without spike bleed flow. As can be interpreted from Fig. 12, spike bleed flow was more effective at below-nominal values of corrected airflow. The data also show that spike bleed flow decreased the inlet stability margin.

(8) Subsequent isolated inlet testing was done with spike bleed pattern 6 operating at maximum bleed flow rate. The optimum spike position was established as $X/R = 1.63$ for a corrected airflow of 180 lb_m/sec at Mach number 2.06.

4.1.2 Mutual Interference Effects

(8) The mutual interference effects of the nonstaggered dual-inlet installations are shown in Fig. 13. These data were obtained by setting a desired performance for one of the inlets and varying the mass flow of the other inlet. For clarity the inlets were identified, as they were

~~SECRET~~
DECLASSIFIED / UNCLASSIFIED

~~SECRET~~**DECLASSIFIED / UNCLASSIFIED**

commonly referred to when attached to the AMSA model, as either the inboard inlet or the outboard inlet. For the three inlet spacings investigated the inboard inlet performance was not degraded as the outboard inlet mass flow was throttled to the stability limit. As the outboard inlet mass flow was throttled past the stability limit, the inboard inlet performance became slightly sensitive to inlet spacing only when the inboard inlet was set for a below-nominal corrected airflow of $170 \text{ lb}_m/\text{sec}$. Flow distortion was unaffected at all test conditions.

(6) The interference effects of staggering the outboard inlet 3.5 inlet diameters downstream of the inboard inlet are shown in Fig. 14. Varying the outboard mass flow had no effect on inboard inlet performance; however, varying the inboard mass flow caused outboard inlet recovery degradation of approximately 2 percent at nominal corrected airflow and approximately 4.5 percent at a below-nominal corrected airflow of $165 \text{ lb}_m/\text{sec}$. Flow distortion was unaffected for the inboard inlet and was increased slightly for the outboard inlet when the inboard inlet mass flow was throttled past the stability limit.

(7) The dual-inlet configuration selected as the best compromise installation for the inlet-airplane phase of testing was the nonstaggered dual-inlet configuration having the 0.84-inlet-diameter spacing.

4.2 INLET-AIRPLANE TESTS**4.2.1 Effect of Spike Position**

(6) The effect of spike position on both the inboard and outboard inlet performance at Mach numbers from 0.85 to 2.20 at an angle of attack of 5 deg is shown in Fig. 15. The data, presented at constant corrected airflows, were within $\pm 2 \text{ lb}_m/\text{sec}$ of the previously defined nominal corrected airflow for the respective Mach numbers. The data were used to select the spike positions for optimum inlet performance at the assumed cruise angle of attack of 5 deg. The effect of second-cone deflection angle on inlet performance at Mach numbers of 0.85 and 1.20 is also shown. Collapsing the second-cone deflection angle from 15 to 10 deg, at the spike position for optimum inlet performance, improved recovery approximately 0.3 percent at $M_\infty = 0.85$ and 0.6 percent at $M_\infty = 1.20$. At Mach numbers from 1.75 to 2.20 the spike position for optimum outboard inlet performance was at a slightly more extended position than that for the inboard inlet. The discrepancy is believed to be caused by slightly different spike and cowl contours of the two inlets since the discrepancy also appeared during the isolated inlet phase of testing.

DECLASSIFIED / UNCLASSIFIED~~SECRET~~

DECLASSIFIED / UNCLASSIFIED

4.2.2 Effect of Spike Bleed Flow

(S) Limited data were obtained for determining the effect of spike bleed flow on inlet performance. At Mach numbers of 0.85 and 1.20, the spikes contained no perforations to bleed the boundary layer. In general the spike bleed plugs were fully open at the supersonic Mach number conditions investigated. However, the effect of spike bleed was investigated at $M_\infty = 2.20$ at the assumed cruise angle of attack of 5 deg. The data presented in Fig. 16 show that recovery was unaffected for spike bleed flow greater than approximately 2 percent of the inlet capture flow. Spike bleed mass-flow ratio above 0.02 increased recovery approximately 2 percent at $M_\infty = 2.20$ at the cruise angle of attack of 5 deg.

4.2.3 Effects of Angle of Attack and Sideslip

(S) The effects of angle of attack and sideslip on inlet performance, for previously defined corrected airflows at optimum spike settings, are shown in Figs. 17 and 18, respectively. The inboard inlet performance was more sensitive to model attitude than was the outboard inlet. At Mach numbers of 1.75, 2.05, and 2.20, the maximum recovery and minimum distortion occurred at angles of attack greater than the 5-deg cruise angle of attack. To move the peak recovery points closer to the 5-deg cruise angle of attack, the data indicate that the inlets should be pitched up to align the inlets to the local flow angularity. As would be expected at positive angles of sideslip, recovery decreased and distortion increased because the inlets were in the flow field wake generated by the fuselage.

4.2.4 Optimum Inlet Performance

(S) Figure 19 shows a summary of the optimum inboard and outboard inlet performance for a 5-deg cruise angle of attack over the Mach number range investigated. Optimum recovery varied from 0.99 at $M_\infty = 0.85$ to 0.88 at $M_\infty = 2.20$ while total-pressure distortion remained at or below 0.1 through the Mach number range.

(S) Also shown in Fig. 19 is the isolated inlet performance at the same corrected airflows and spike settings as were determined at the respective Mach numbers for the inlet-airplane phase of testing. The increase in performance shown for the inlet-airplane configuration at Mach numbers greater than 1.20 results from a decrease in the local Mach number ahead of the inlets which was generated by the weak oblique shock system of the wing-fuselage combination, thereby decreasing the total-pressure losses associated with the inlet shock system.

DECLASSIFIED / UNCLASSIFIED

DECLASSIFIED / UNCLASSIFIED**SECTION V
CONCLUSIONS**

(U) A summary of the significant test results of the wind tunnel investigation of a 1/8-scale AMSA inlet model in Tunnel 16T and Tunnel 16S is as follows:

- (S) 1. The nonstaggered, dual-isolated inlet configurations had no mutual inlet interaction effects at nominal corrected airflow at free-stream Mach number 2.06.
- (S) 2. The outboard inlet performance was adversely affected by the inboard inlet performance for the staggered, dual-isolated inlet configuration at free-stream Mach number 2.06.
- (S) 3. Inboard inlet performance was more sensitive to airplane attitude than was the outboard inlet.
- (S) 4. Maximum inlet performance did not occur at predicted airplane cruise attitude for the Mach number range from 1.75 to 2.20.

DECLASSIFIED / UNCLASSIFIED

APPENDIXES
I. ILLUSTRATIONS
II. TABLE

SECRET

DECLASSIFIED / UNCLASSIFIED

AEDC-TR-67-252

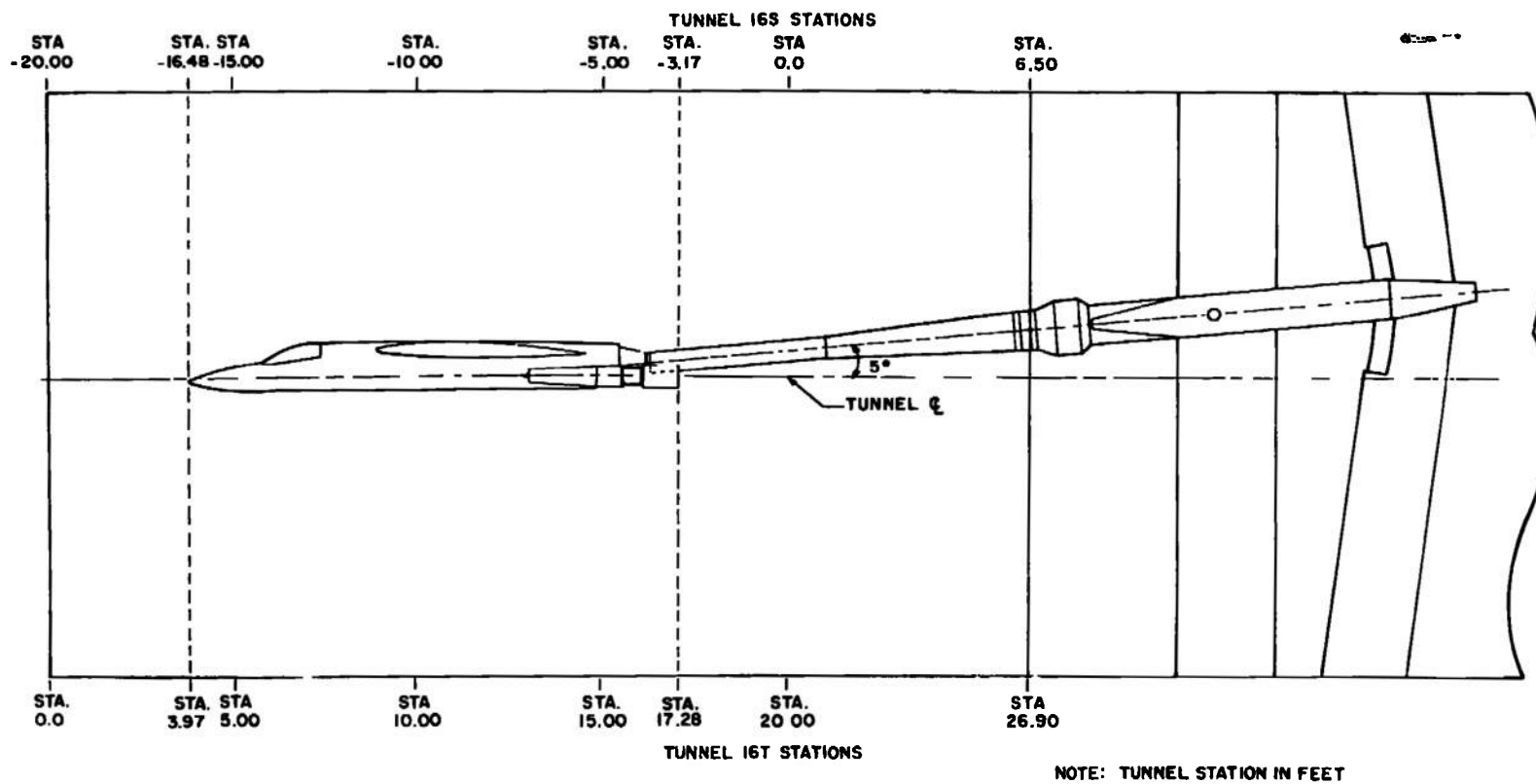
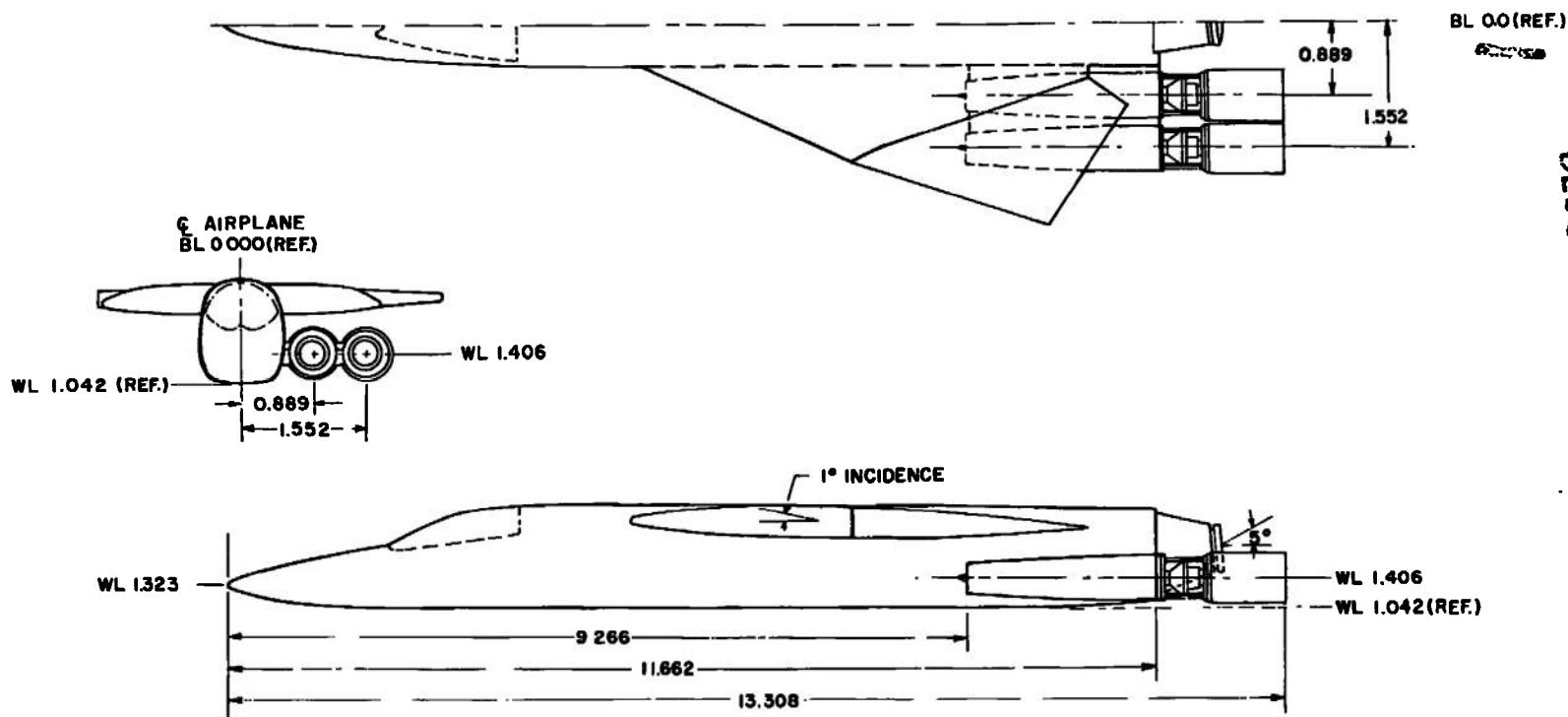


Fig. 1 Location of AMSA 1/8-Scale Inlet Model in Tunnel 16T and Tunnel 16S Test Sections

DECLASSIFIED / UNCLASSIFIED

DECLASSIFIED / UNCLASSIFIED



DIMENSIONS ARE IN FEET

SECRET

Fig. 2 Sketch of AMSA 1/8-Scale Inlet Model

DECLASSIFIED / UNCLASSIFIED

12

DECLASSIFIED / UNCLASSIFIED

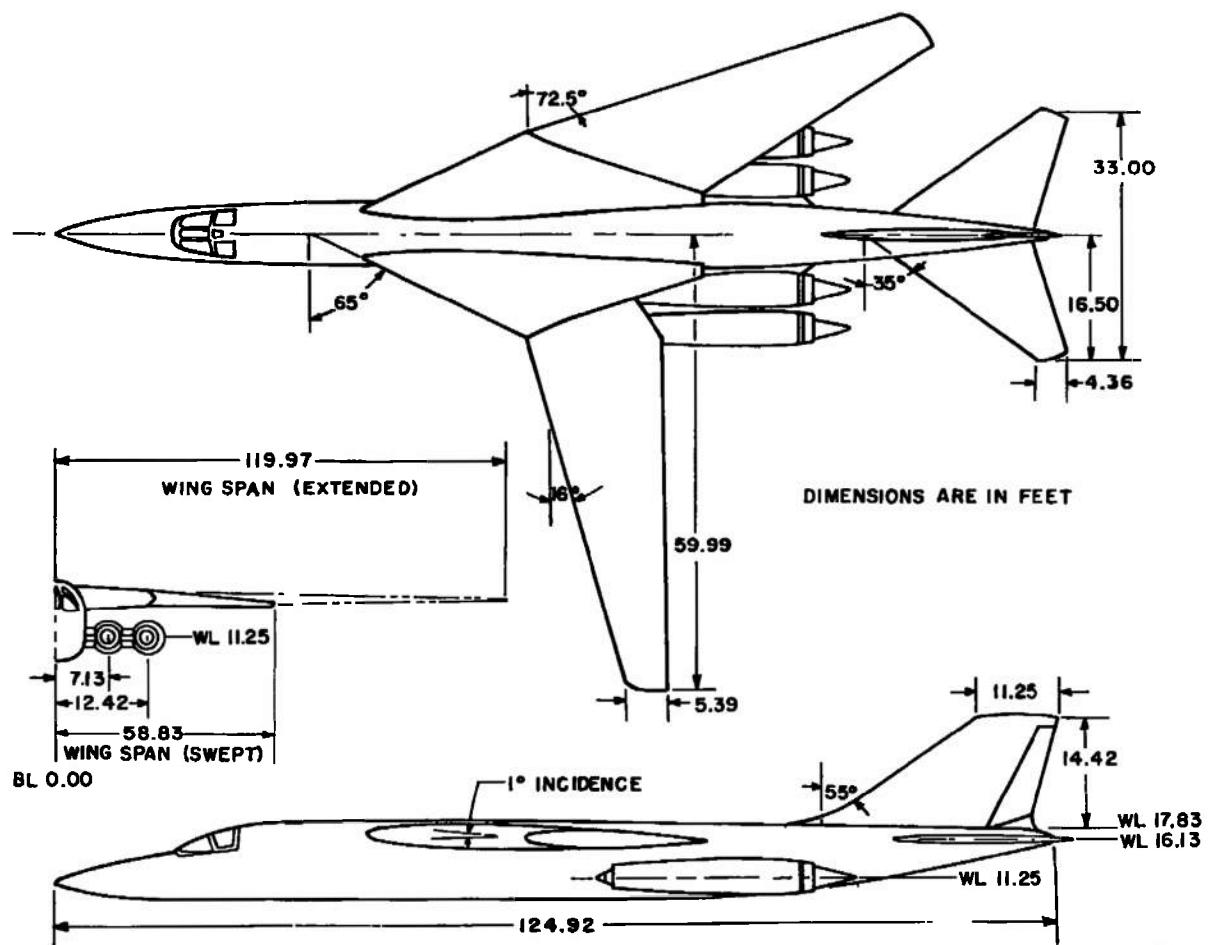
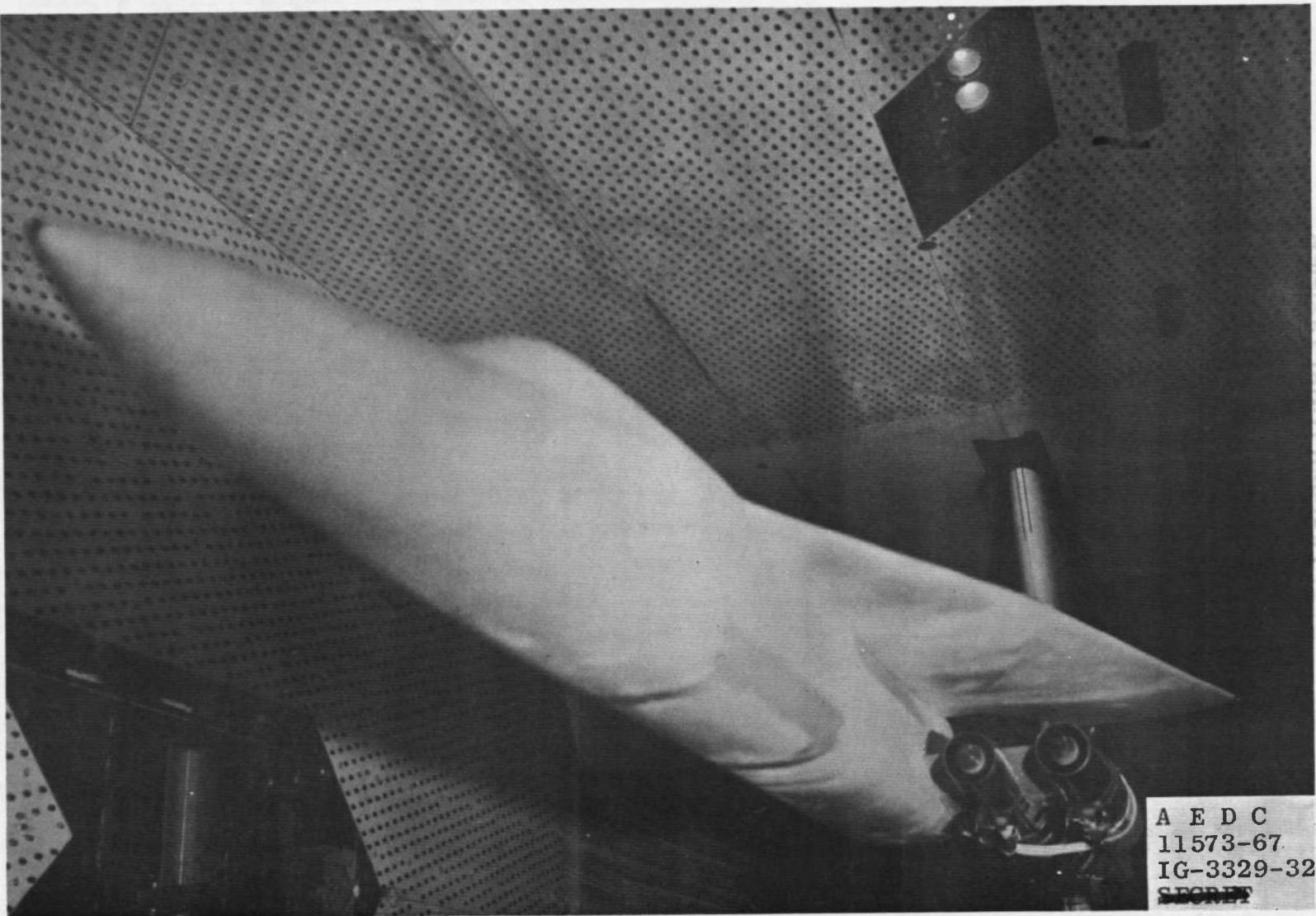


Fig. 3 Sketch of the Proposed AMSA

DECLASSIFIED / UNCLASSIFIED

DECLASSIFIED / UNCLASSIFIED

~~SECRET~~



a. Tunnel 16T

Fig. 4 Inlet Airplane Model Installation in Test Section

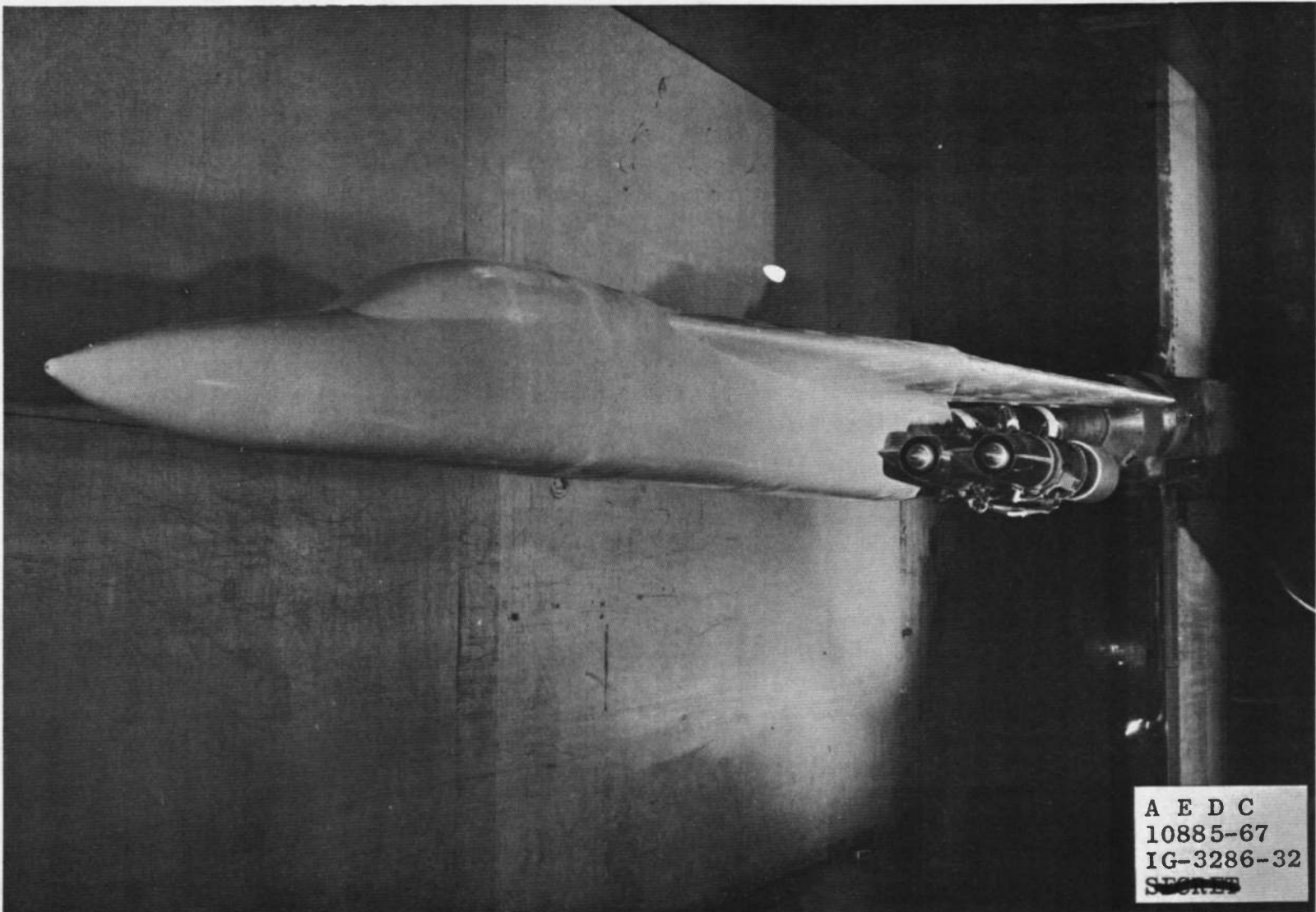
DECLASSIFIED / UNCLASSIFIED

~~SECRET~~

~~SECRET~~

DECLASSIFIED / UNCLASSIFIED

AEDC-TR-67-252



b. Tunnel 16S
Fig. 4 Concluded

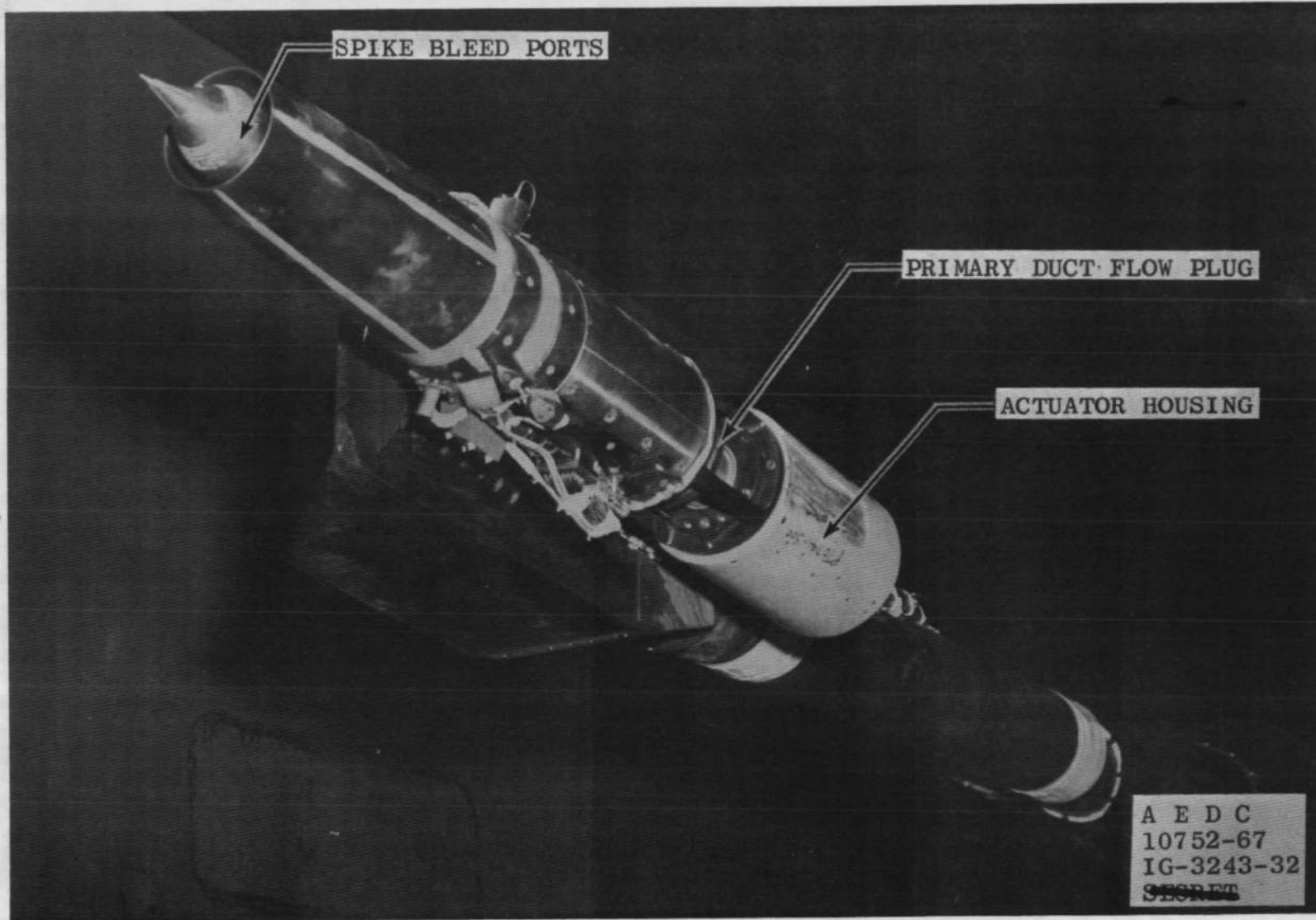
15 DECLASSIFIED / UNCLASSIFIED

~~SECRET~~

SECRET

DECLASSIFIED / UNCLASSIFIED

Q37122AJ000 / Q37122AJ030



a. Single Inlet

Fig. 5 Isolated Inlet Installation in Test Section

DECLASSIFIED / UNCLASSIFIED

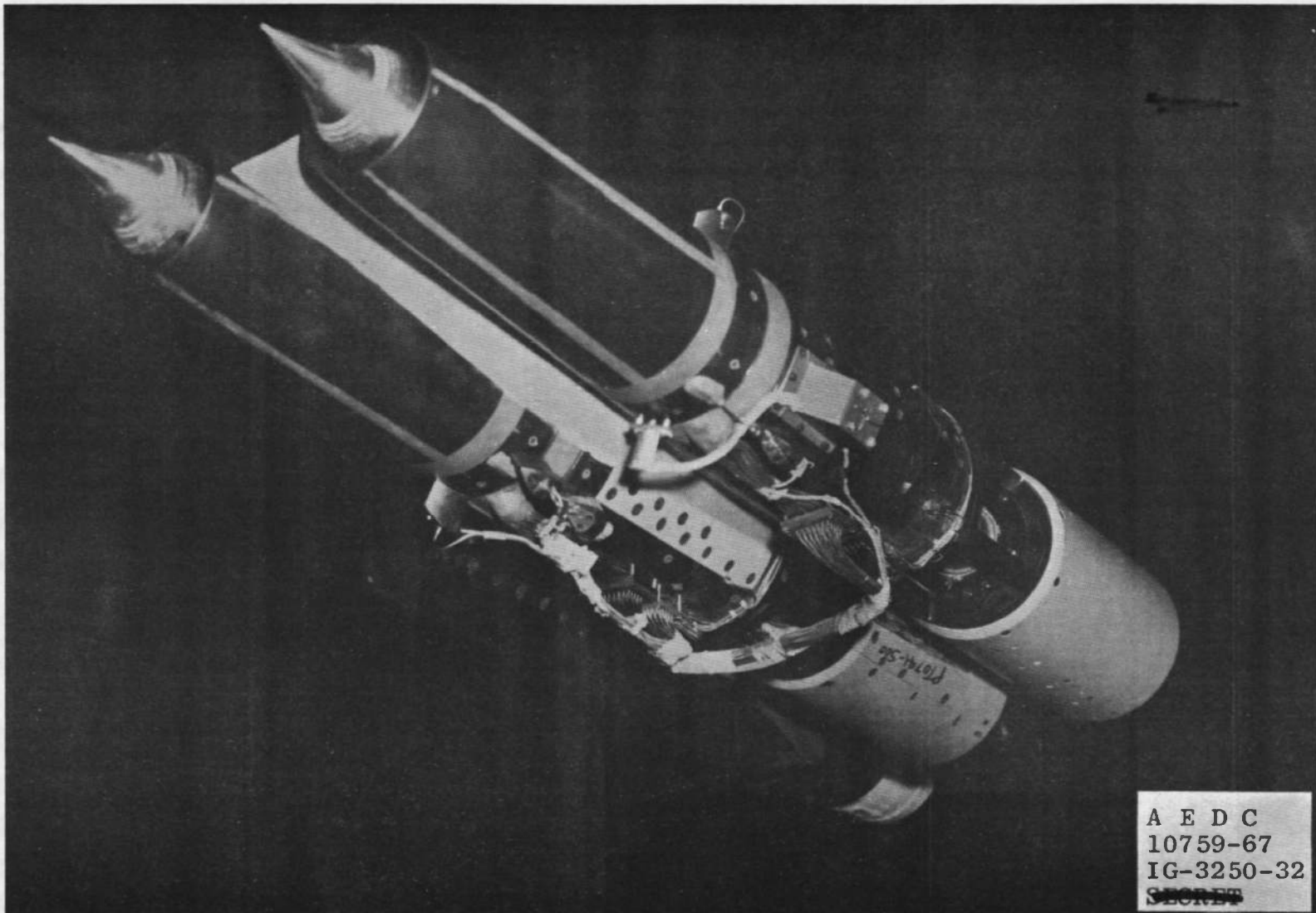
Q37122AJ000 / Q37122AJ030

SECRET

~~SECRET~~

AEDC-TR-67-252

DECLASSIFIED / UNCLASSIFIED



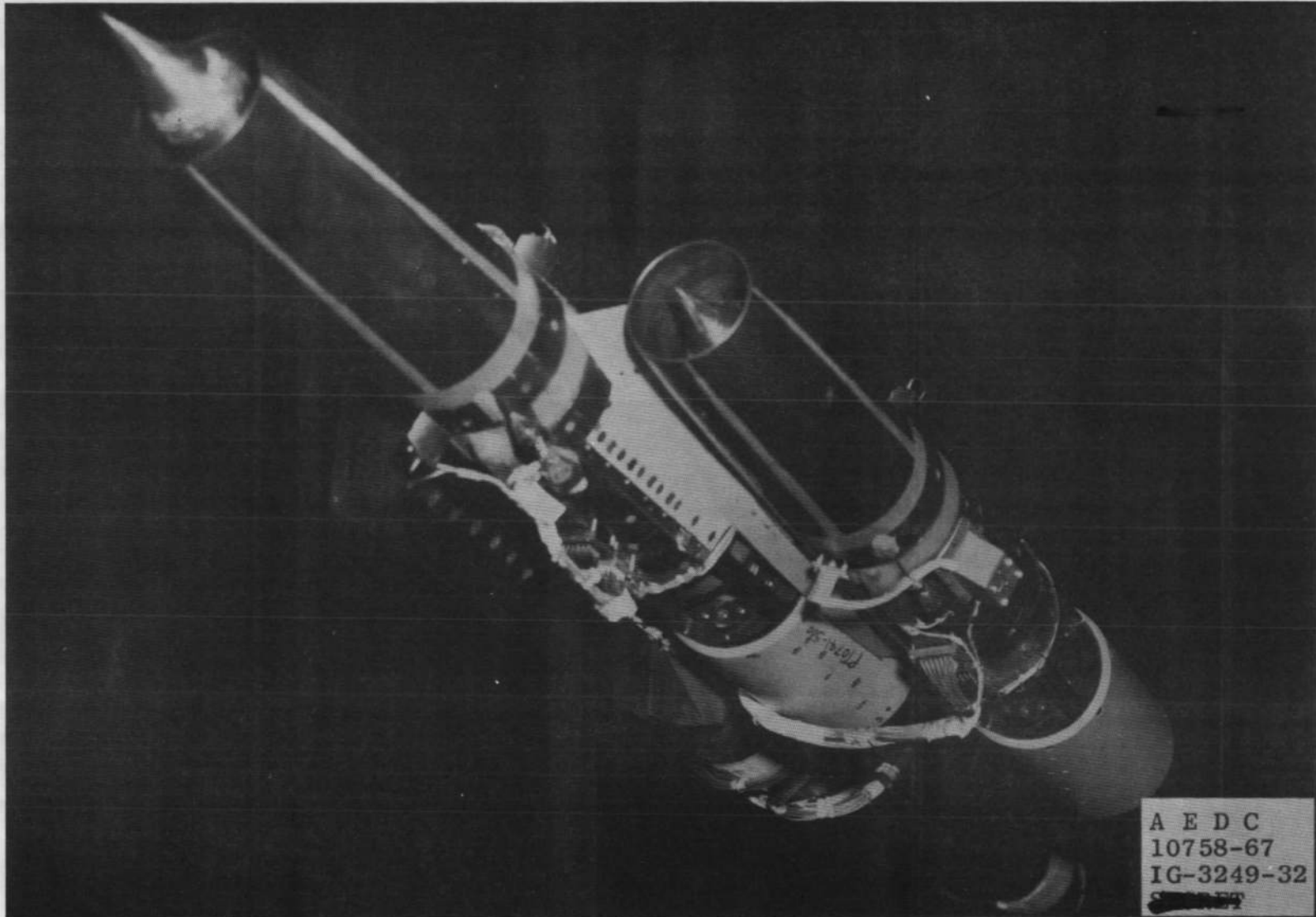
b. Dual Inlets: Nonstaggered Arrangement

Fig. 5 Continued

DECLASSIFIED / UNCLASSIFIED

~~SECRET~~

DECLASSIFIED / UNCLASSIFIED

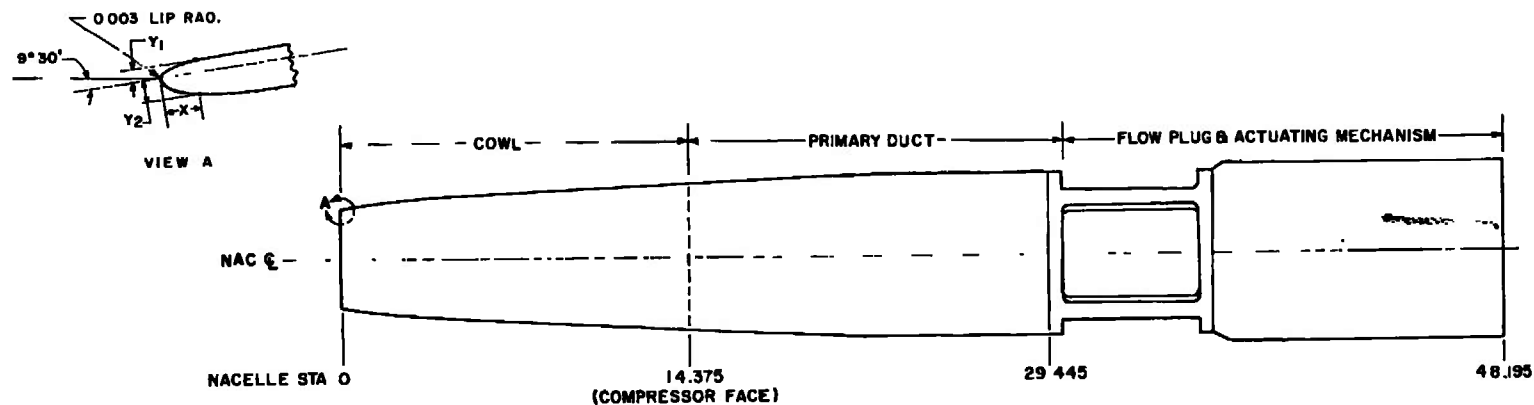


c. Dual Inlets: Staggered Arrangement
Fig. 5 Concluded

DECLASSIFIED / UNCLASSIFIED

DECLASSIFIED / UNCLASSIFIED

19



NACELLE GEOMETRY

NACELLE STATION	INTERNAL RAO	EXTERNAL RAO
0.0	2.176	2.176
0.281	2.161	2.249
0.625	2.209	2.293
1.250	2.263	2.364
1.675	2.301	2.423
2.500	2.334	2.476
3.125	2.359	2.525
3.750	2.381	2.566
4.375	2.403	2.601
5.000	2.421	2.635
5.625	2.440	2.664
6.250	2.456	2.694
6.875	2.471	2.721
7.500	2.484	2.750
8.125	2.496	2.781
8.750	2.505	2.806
9.375	2.515	2.835
10.000	2.528	2.864
10.625	2.535	2.891
11.250	2.544 *	2.920
11.875	↓	2.949
12.000		2.794
13.125		3.003
13.750		3.029
14.375		3.066
15.375	2.544 *	—
16.375	2.646 *	—
22.075	2.646 *	3.395 *
29.445	2.646 *	3.395 *

NACELLE LIP (VIEW A-A)		
X	Y1	Y2
0.0	0.0	0.0
0.013	0.012	0.020
0.025	0.016	0.029
0.050	0.022	0.039
0.075	0.025 *	0.046
0.125	0.025 *	0.054
0.138	0.025 *	—
0.188	—	0.056
0.250	—	0.058 *
0.270	—	0.058 *

* INDICATES POINTS ON STRAIGHT LINE

DIMENSIONS ARE IN INCHES

Fig. 6 Dimensioned Sketch of Model Nacelle

DECLASSIFIED / UNCLASSIFIED

AEDC-TR-67-252

SECRET

DECLASSIFIED / UNCLASSIFIED

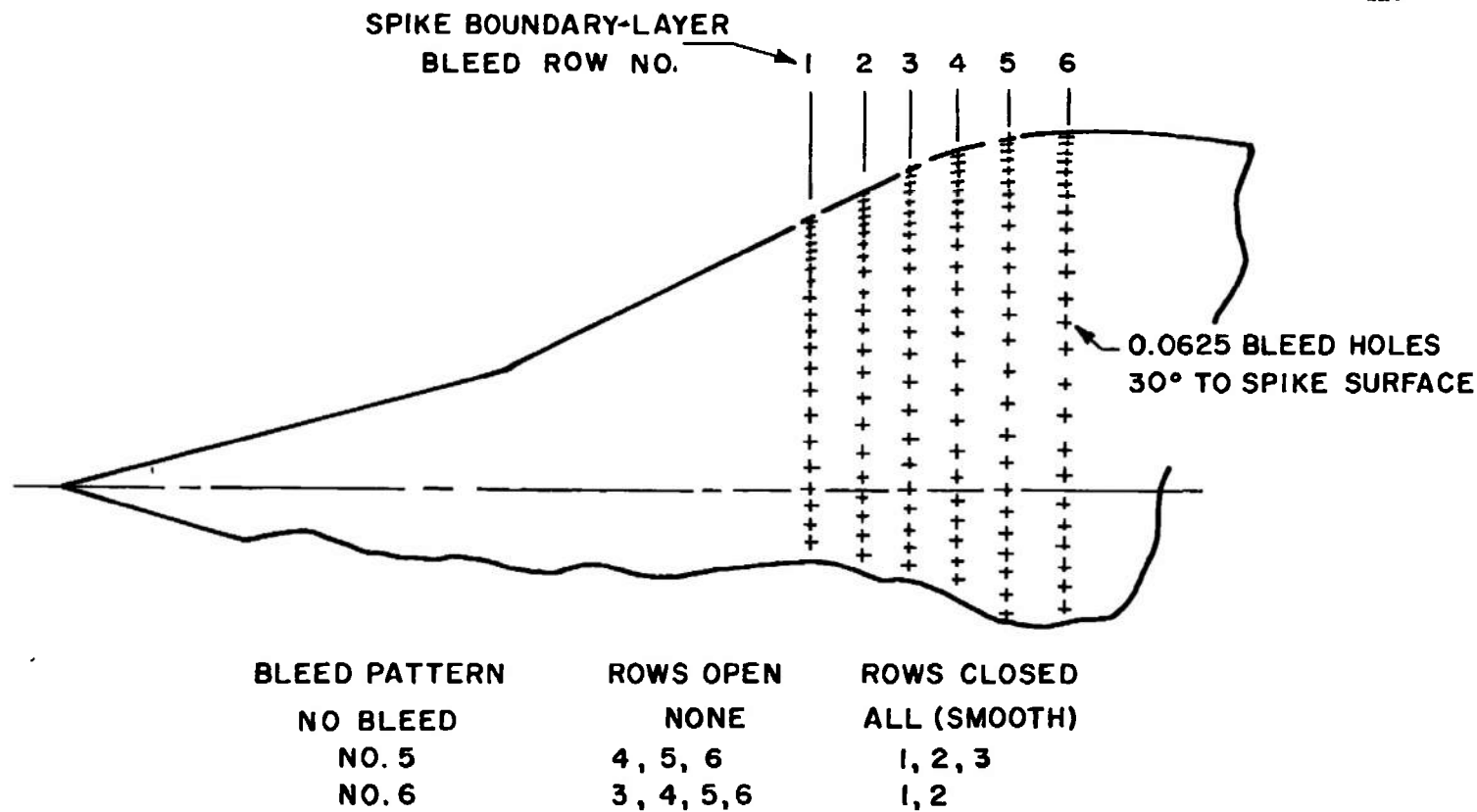
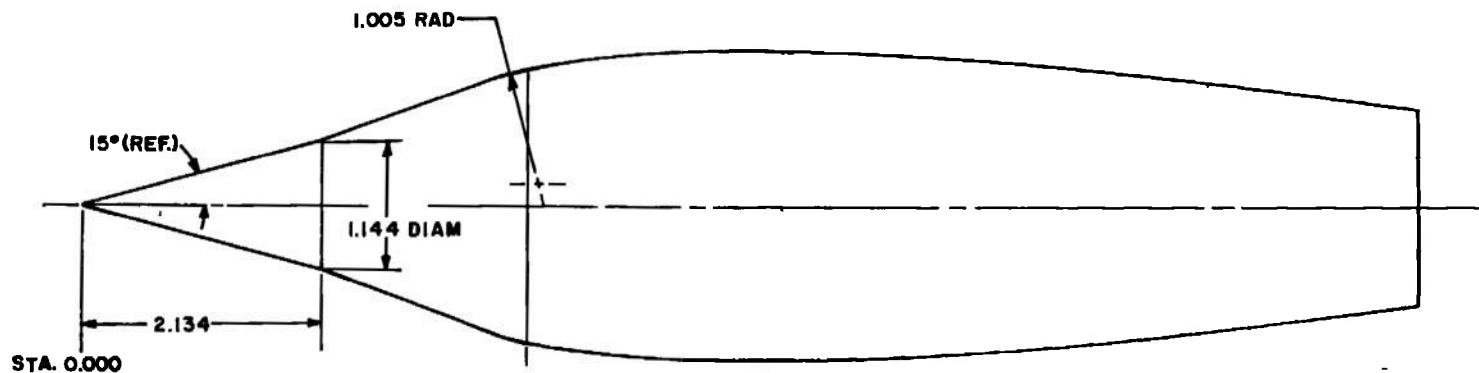


Fig. 7 Spike Boundary-Layer Bleed Pattern

SECRET

DECLASSIFIED / UNCLASSIFIED

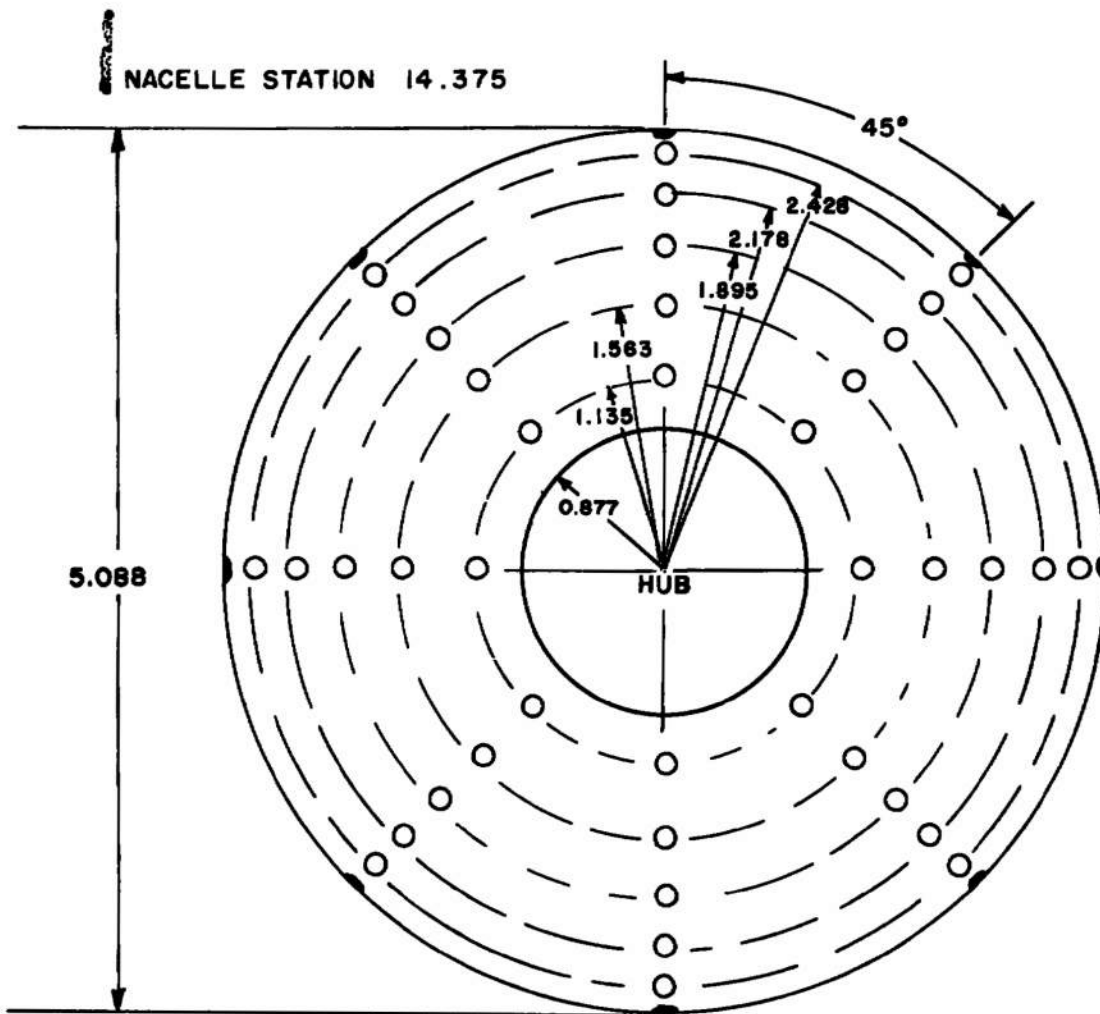


10		15		20		24		27	
I ₁		I ₁		I ₁		I ₁		I ₁	
STA	RAD	STA	RAD	STA	RAD	STA	RAD	STA	RAD
+0.0	0.0	+0.0	0.0	+0.0	0.0	+0.0	0.0	+0.0	0.0
+2.134	0.572	+2.134	0.572	+2.134	0.572	+2.134	0.572	+2.134	0.572
+3.806	0.867	+3.775	1.012	+3.731	1.191	+3.686	1.263	+3.648	1.343
*4.046	0.881	*4.018	1.045	*3.960	1.205	*3.915	1.333	*3.873	1.429
4.106	0.898	4.106	1.066	4.106	1.241	4.106	1.374	4.106	1.479
4.710	1.019	4.710	1.171	4.710	1.325	4.710	1.441	4.710	1.533
5.335	1.084	5.335	1.224	5.335	1.360	5.335	1.466	5.335	1.551
5.960	1.121	5.960	1.250	5.960	1.373	5.960	1.470	5.960	1.544
6.585	1.141	6.585	1.256	6.585	1.366	6.585	1.451	6.585	1.516
7.210	1.143	7.210	1.246	7.210	1.341	7.210	1.416	7.210	1.475
7.835	1.130	7.835	1.219	7.835	1.303	7.835	1.370	7.835	1.416
8.460	1.109	8.460	1.184	8.460	1.254	8.460	1.310	8.460	1.350
9.085	1.075	9.085	1.136	9.085	1.196	9.085	1.244	9.085	1.271
9.710	1.035	9.710	1.084	9.710	1.129	9.710	1.169	9.710	1.189
10.335	0.988	10.335	1.025	10.335	1.059	10.335	1.086	10.335	1.100
10.960	0.940	10.960	0.966	10.960	0.987	10.960	1.000	10.960	1.011
11.585	0.894	11.585	0.905	11.585	0.921	11.585	0.916	11.585	0.924
11.951	0.864	11.975	0.864	11.918	0.864	11.980	0.864	12.043	0.864

NOTE:
 STRAIGHT LINE BETWEEN
 POINTS MARKED ++,
 1.005 RAD. BETWEEN POINTS
 MARKED + *,
 SHARP BREAK AT POINT
 MARKED * EXCEPT ON I₁ 27

DIMENSIONS ARE IN INCHES

Fig. 8 Inlet Spike Contours

DECLASSIFIED / UNCLASSIFIED**COMPRESSOR-FACE INSTRUMENTATION**

**NOTE: DIMENSIONS
IN INCHES**

**COMPRESSOR FACE
40 TOTAL- PRESSURE PROBES
8 STATIC- PRESSURE TAPS**

**1.875 INCHES FORWARD OF C. F. ON DUCT WALL
1 BUZZ TRANSDUCER AT 157.5°**

UNCLASSIFIED

Fig. 9 Compressor-Face Station Instrumentation

DECLASSIFIED / UNCLASSIFIED

DECLASSIFIED / UNCLASSIFIED

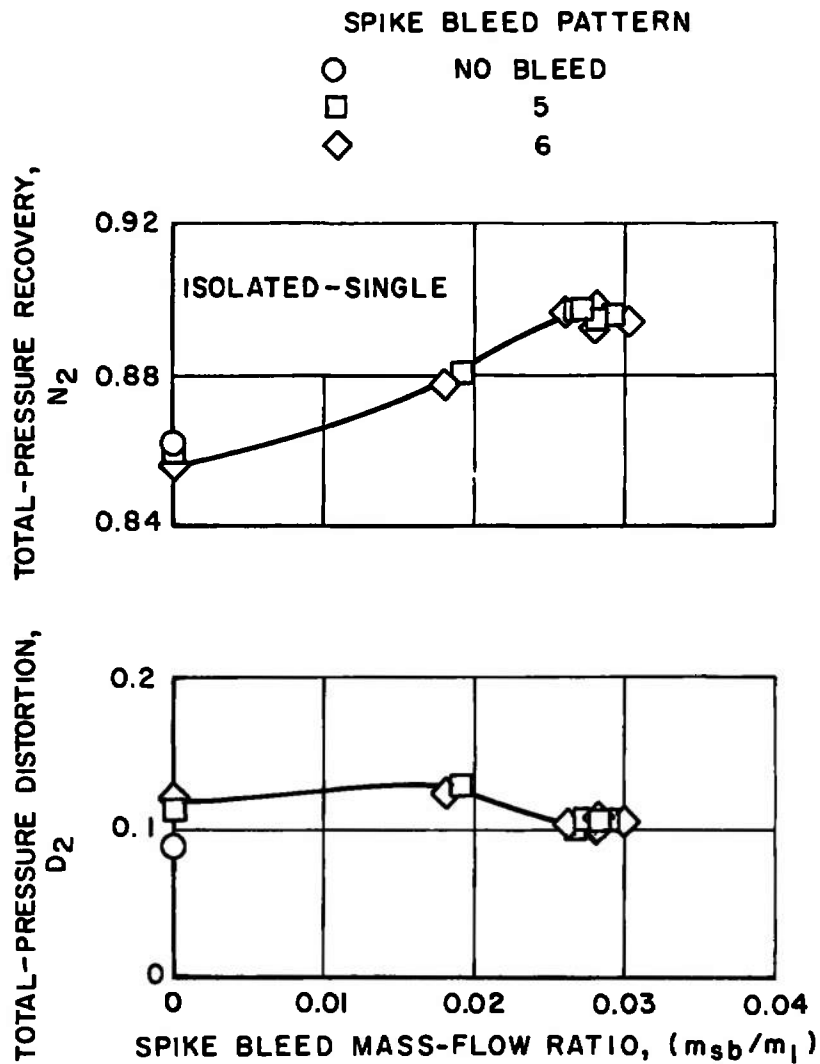


Fig. 10 (8) Effect of Spike Bleed Flow on Inlet Performance, I_1^{27} Spike,
 $M_\infty = 2.06$, $\alpha = 0$ deg, $\beta = 0$ deg, $W \sqrt{\theta/\delta_2} = 185$ lb_m/sec

DECLASSIFIED / UNCLASSIFIED

~~SECRET~~

DECLASSIFIED / UNCLASSIFIED

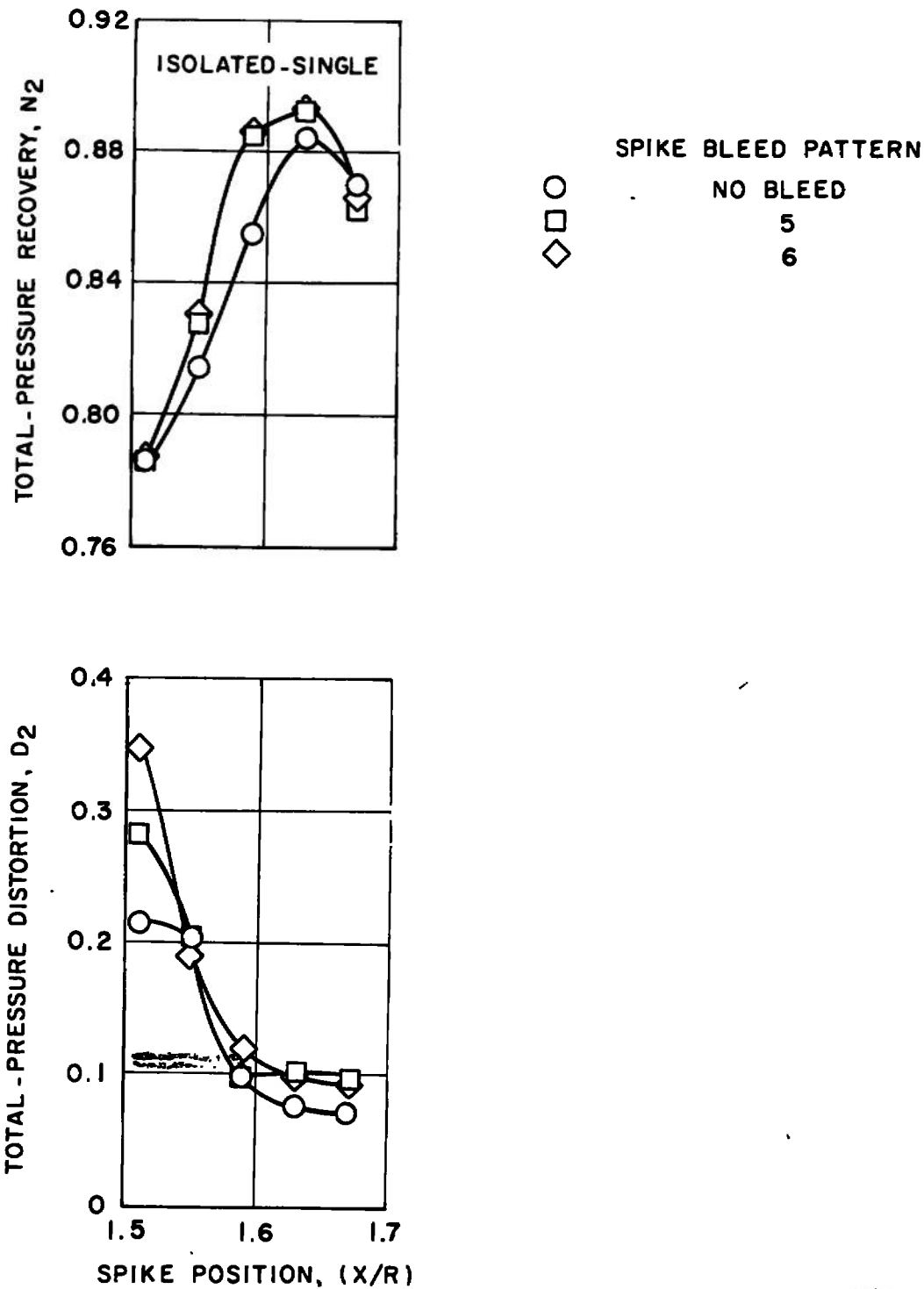


Fig. 11 (b) Effect of Spike Position on Inlet Performance;

 I_1^{27} Spike, $M_\infty = 2.06$, $\alpha = 0^\circ$, $\beta = 0^\circ$, $W\sqrt{\theta}\delta_2 = 180 \text{ lb}_m/\text{sec}$ ~~SECRET~~

DECLASSIFIED / UNCLASSIFIED

DECLASSIFIED / UNCLASSIFIED

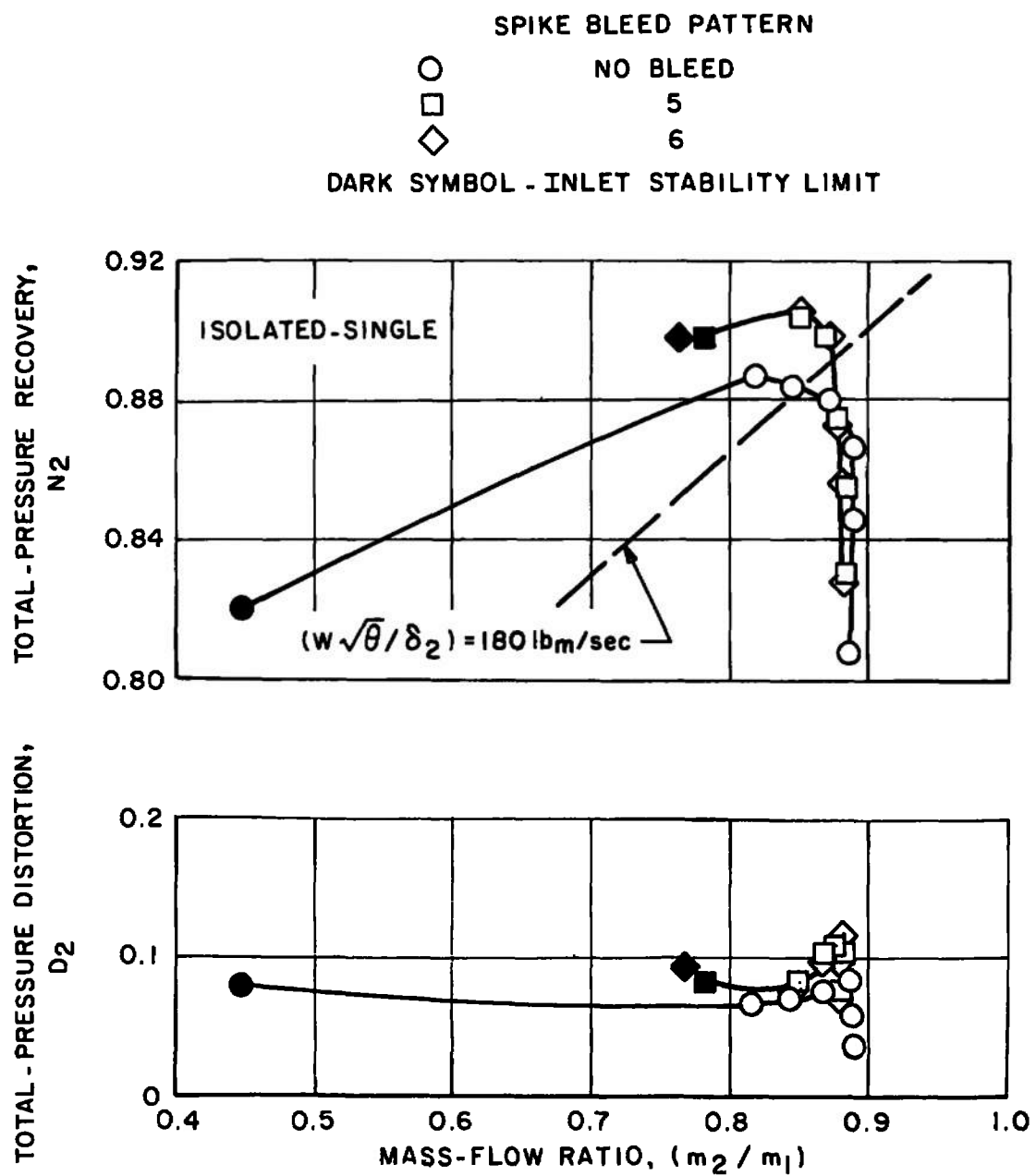


Fig. 12 (b) Effect of Spike Bleed Pattern on Inlet Performance; I_1^{27} Spike, $M_\infty = 2.06$, $\alpha = \text{deg}$, $\beta = 0 \text{ deg}$, $X/R = 1.63$

DECLASSIFIED / UNCLASSIFIED

DECLASSIFIED / UNCLASSIFIED

SECRET

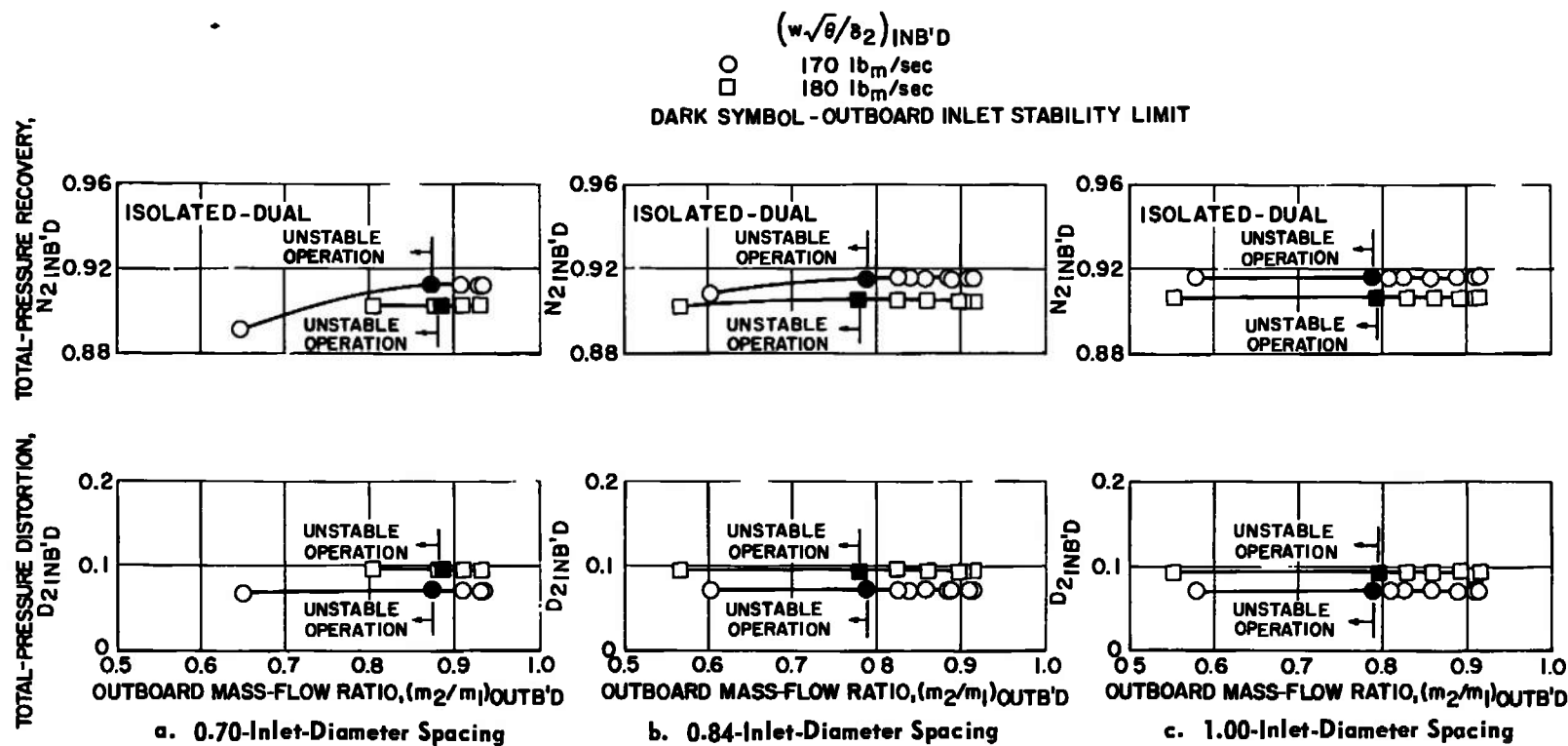


Fig. 13 (2) Mutual Interference Effects of Nonstaggered, Dual-Inlet Orientation on Inlet Performance;
 I_1 27 Spike, $M_\infty = 2.06$, $\alpha = 0$ deg, $\beta = 0$ deg, $X/R = 1.63$

DECLASSIFIED / UNCLASSIFIED

TOTAL-PRESSURE DISTORTION, TOTAL-PRESSURE RECOVERY,

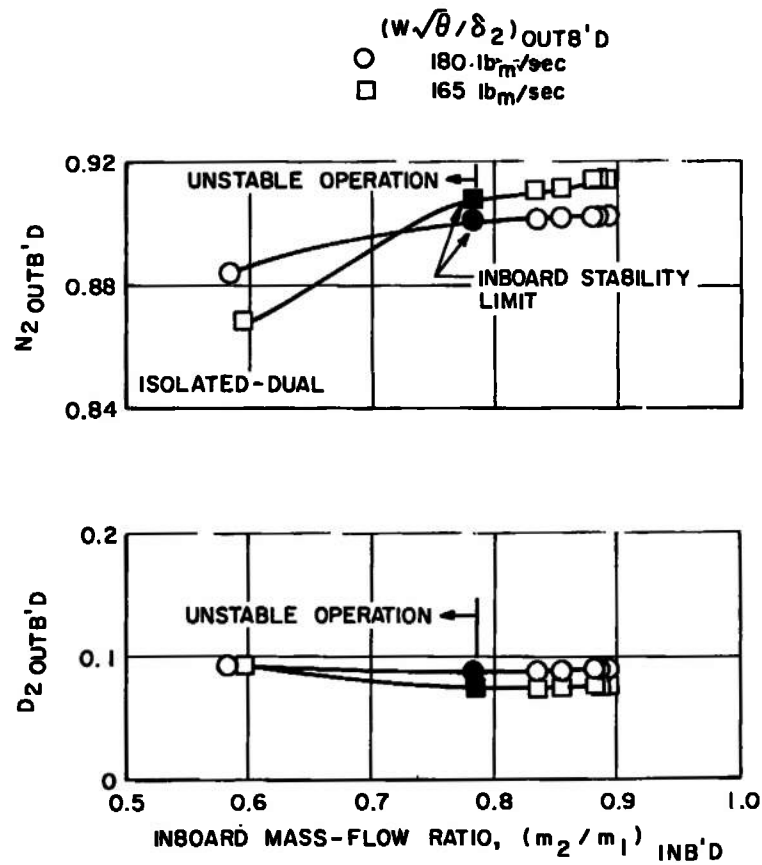
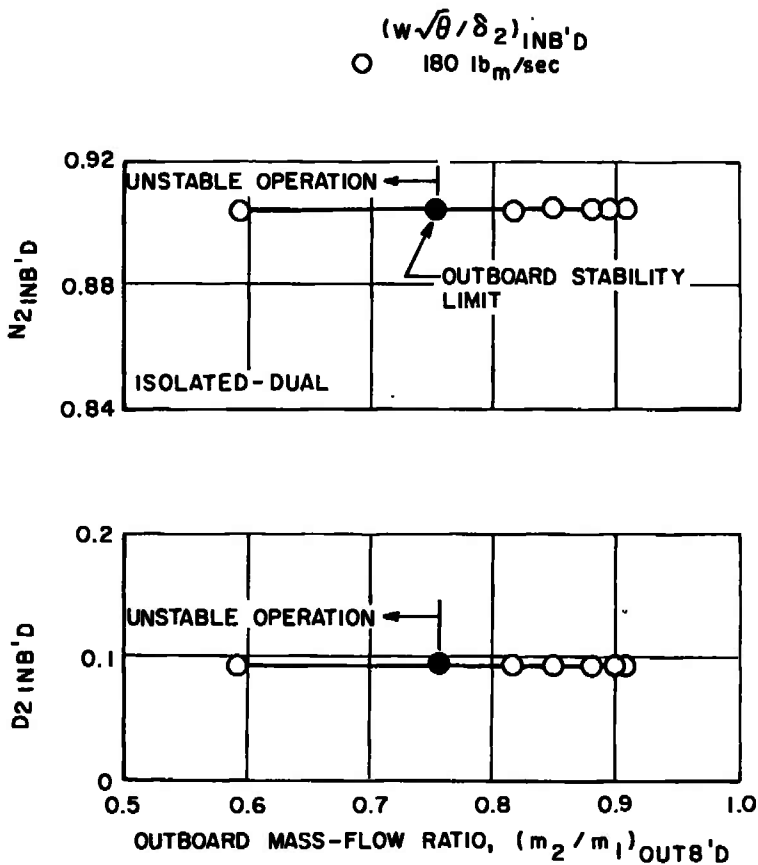
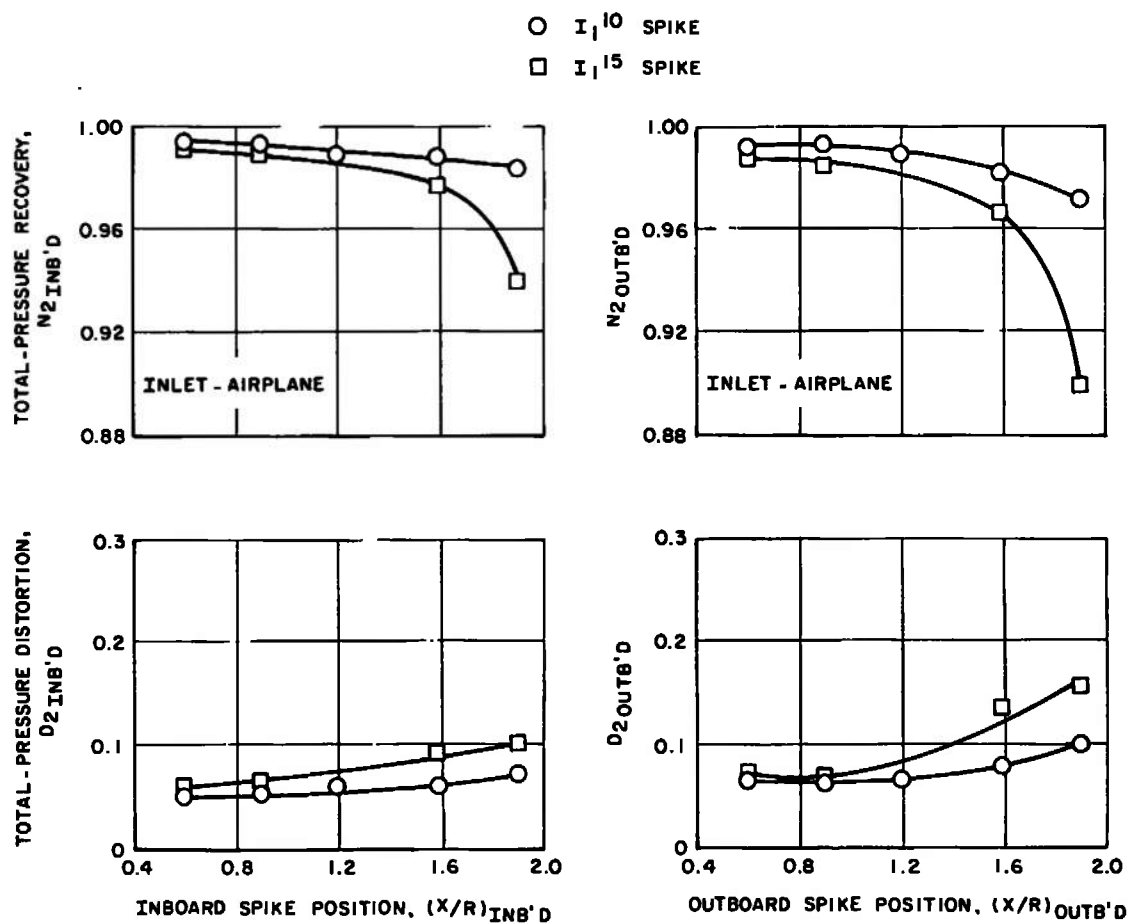


Fig. 14 (8) Mutual Interference Effect of Staggered Dual-Inlet Orientation on Inlet Performance;
 l_1^{27} Spike, $M_\infty = 2.06$, $\alpha = 0$ deg, $\beta = 0$ deg, $(X/R)_{INB'D} = 1.63$, $(X/R)_{OUTB'D} = 1.67$

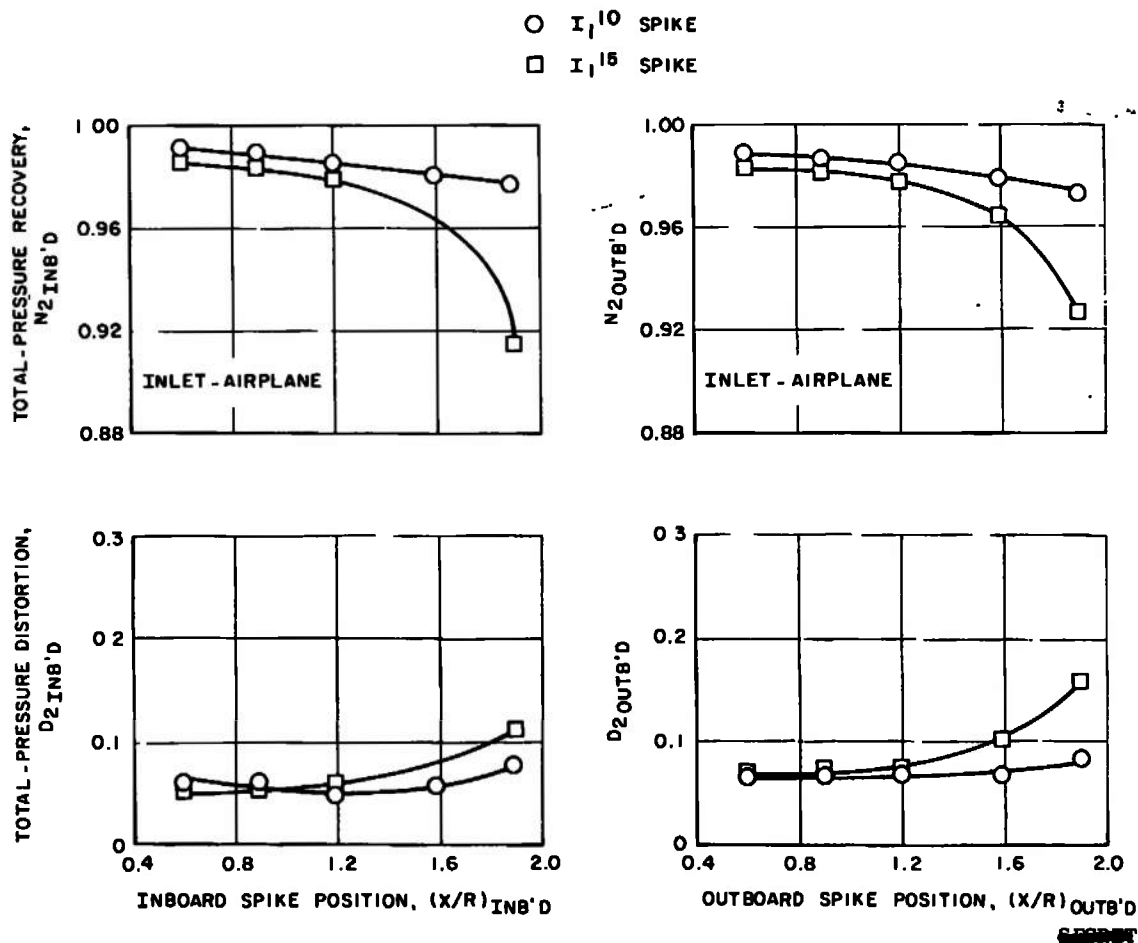
DECLASSIFIED / UNCLASSIFIED



$$\alpha = 5^\circ, M_\infty = 0.85, W\sqrt{\theta/\delta_2} = 260 \text{ lb}_m/\text{sec}$$

Fig. 15 (U) Effect of Spike Position on Inlet Performance; $\alpha = 5^\circ$, $\beta = 0^\circ$

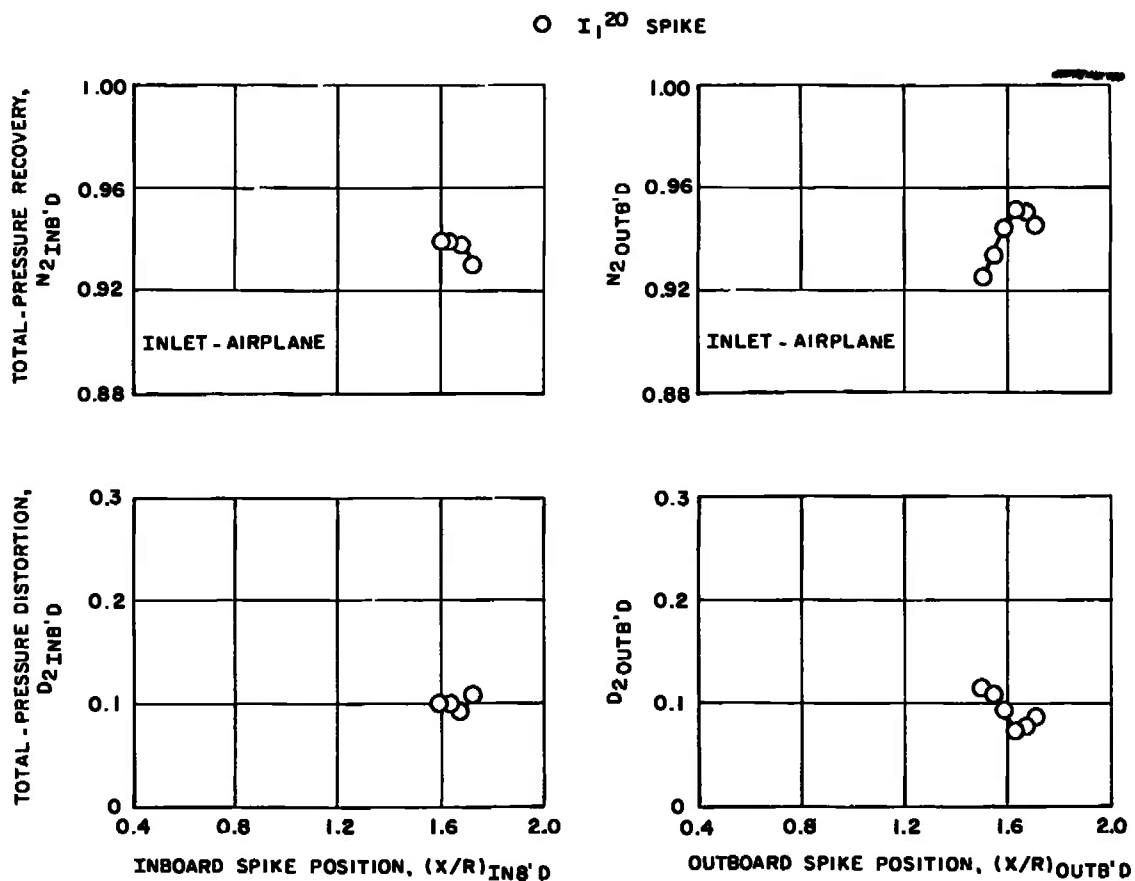
DECLASSIFIED / UNCLASSIFIED



b. $M_{\infty} = 1.20$, $W\sqrt{\theta/\delta_2} = 260 \text{ lb}_m/\text{sec}$

Fig. 15 Continued

DECLASSIFIED / UNCLASSIFIED



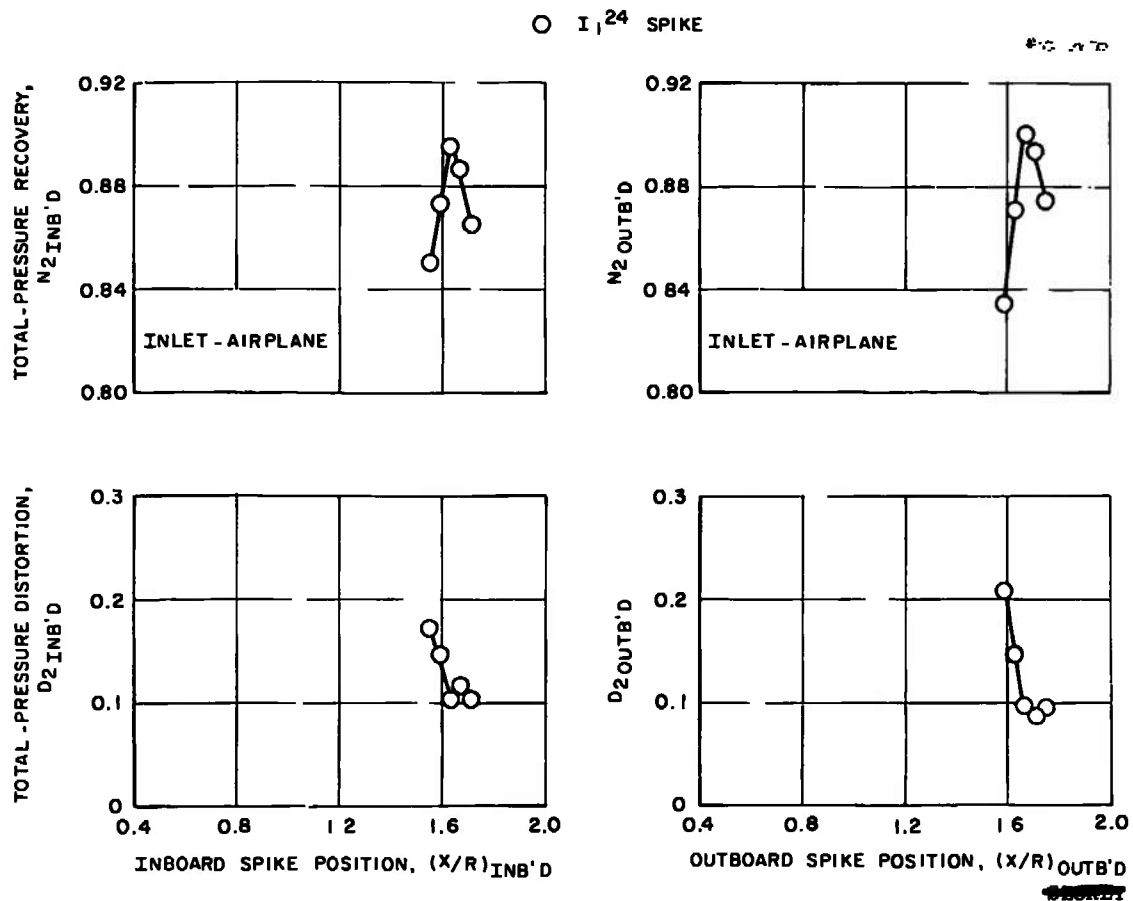
c. $M_{\infty} = 1.75$, $W\sqrt{\theta/\delta_2} = 220 \text{ lb}_m/\text{sec}$

Fig. 15 Continued

DECLASSIFIED / UNCLASSIFIED

DECLASSIFIED / UNCLASSIFIED

AEDC-TR-67-252

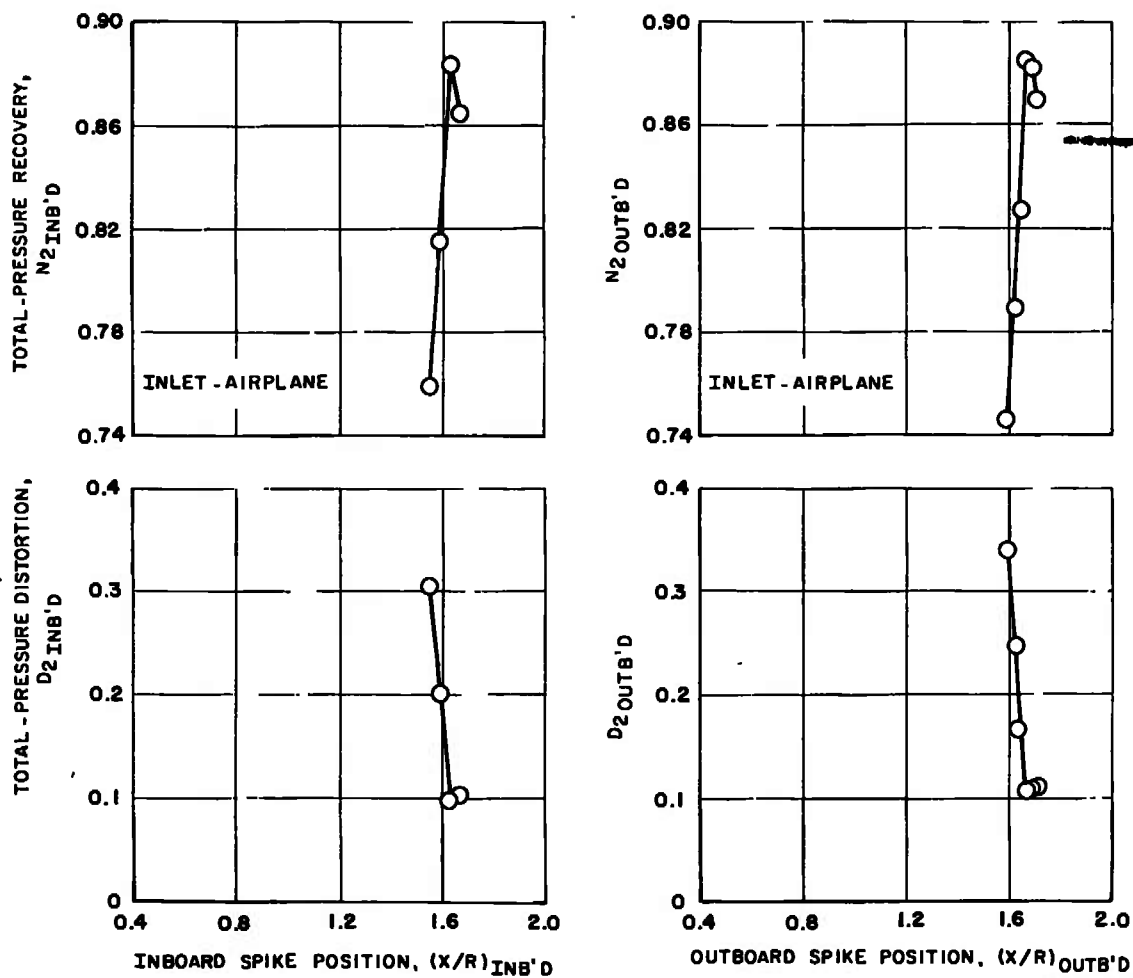


d. $M_\infty = 2.05$, $W\sqrt{\theta/\delta_2} = 196 \text{ lb}_m/\text{sec}$

Fig. 15 Continued

DECLASSIFIED / UNCLASSIFIED

DECLASSIFIED / UNCLASSIFIED

○ I₁²⁷ SPIKE

$$\text{e. (8) } M_{\infty} = 2.20, W\sqrt{\theta/\delta_2} = 180 \text{ lb}_m/\text{sec}$$

Fig. 15 Concluded

DECLASSIFIED / UNCLASSIFIED

DECLASSIFIED / UNCLASSIFIED

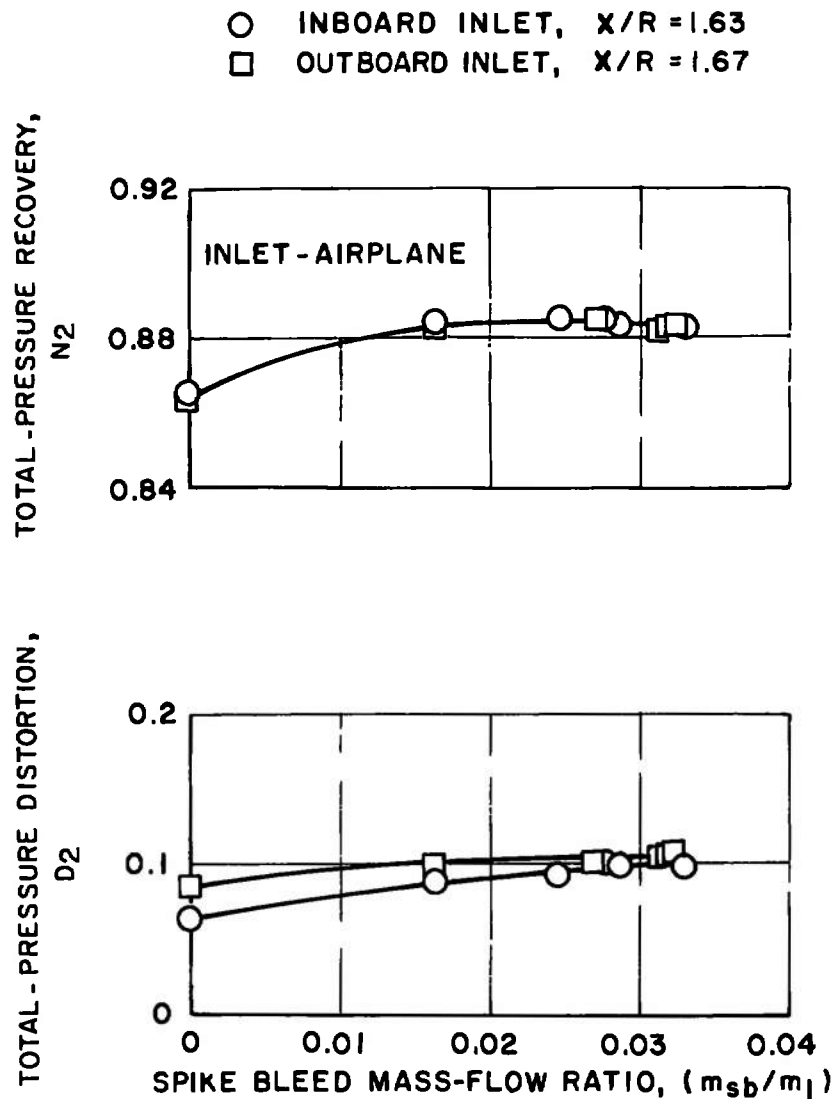


Fig. 16 (8) Effect of Spike Bleed Flow on Inlet Performance;
 $I_{1.27}$ Spike, $M_\infty = 2.20$, $\alpha = +5$ deg, $\beta = 0$ deg,
 $W\sqrt{\theta}/\delta_2 = 180 \text{ lb}_m/\text{sec}$

DECLASSIFIED / UNCLASSIFIED

~~SECRET~~
DECLASSIFIED / UNCLASSIFIED

	M_∞	$w\sqrt{\theta}/b_2$	$(X/R)_{INB'D}$	$(X/R)_{OUTB'D}$	SPIKE
○	0.85	260	0.60	0.60	11
□	1.20	260	0.60	0.60	10
◇	1.75	220	1.60	1.63	20
△	2.05	196	1.63	1.67	24
▽	2.20	180	1.63	1.67	27

DARK SYMBOL - INLET STABILITY LIMIT

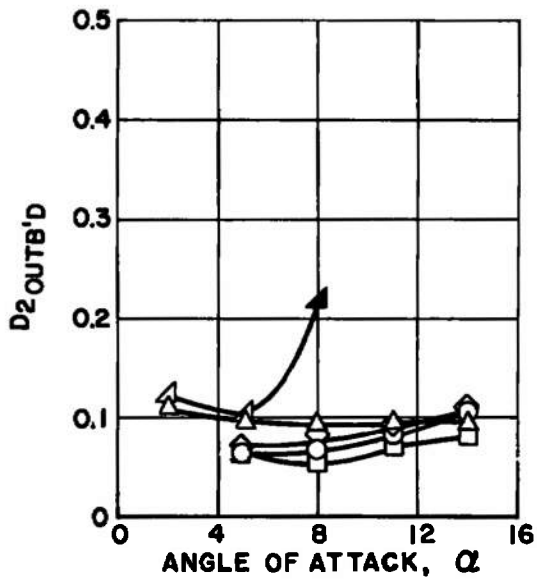
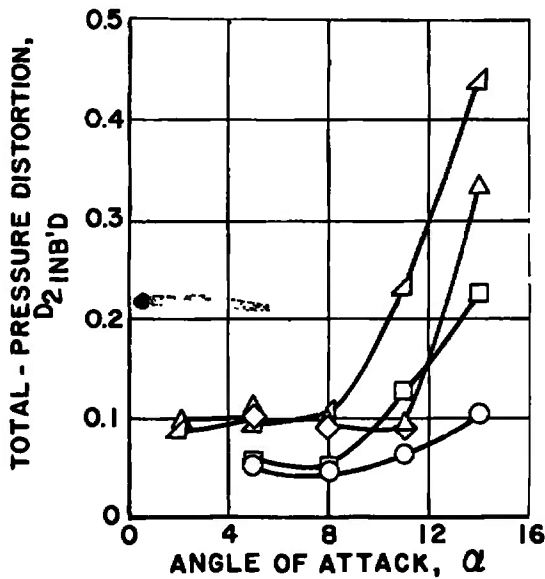
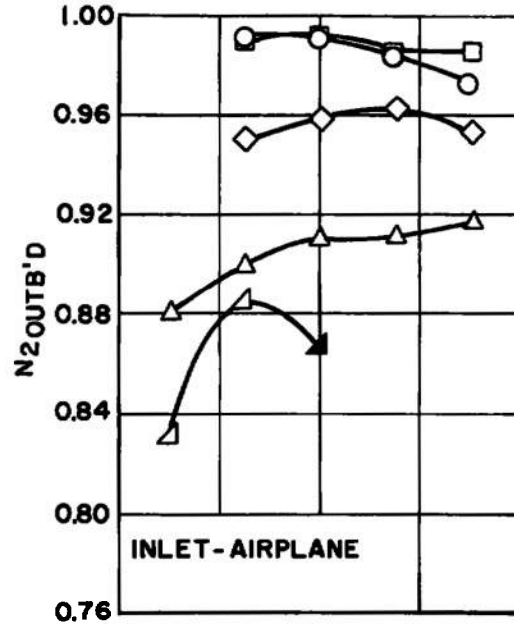
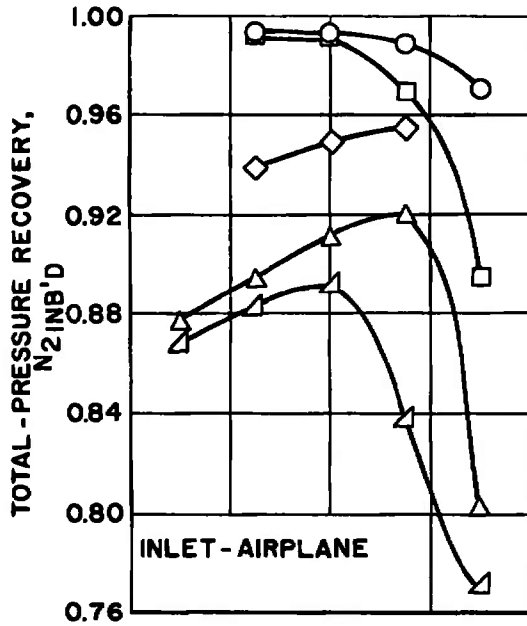
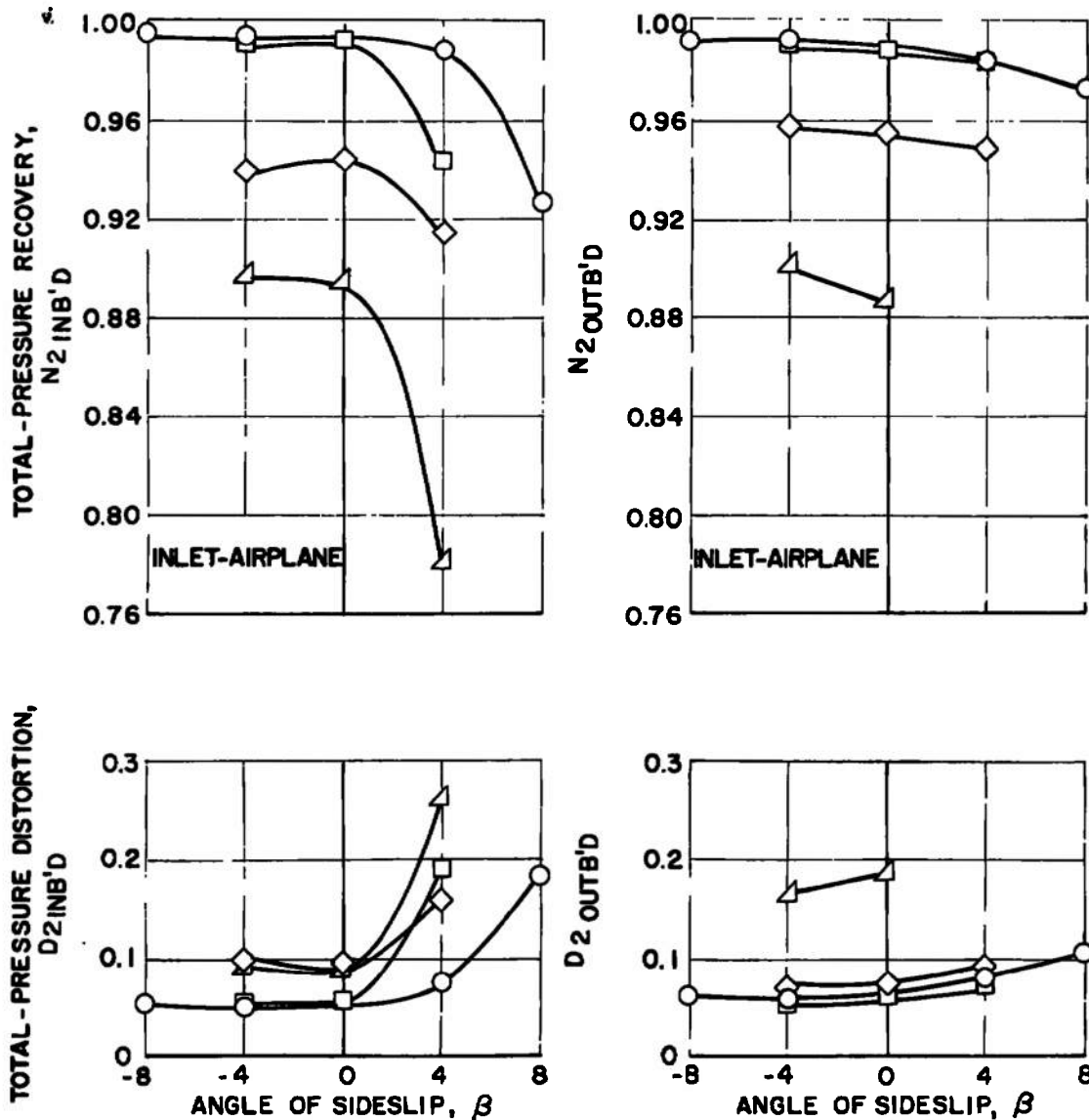


Fig. 17 Effect of Angle of Attack on Inlet Performance; $\beta = 0$ deg

~~SECRET~~
DECLASSIFIED / UNCLASSIFIED

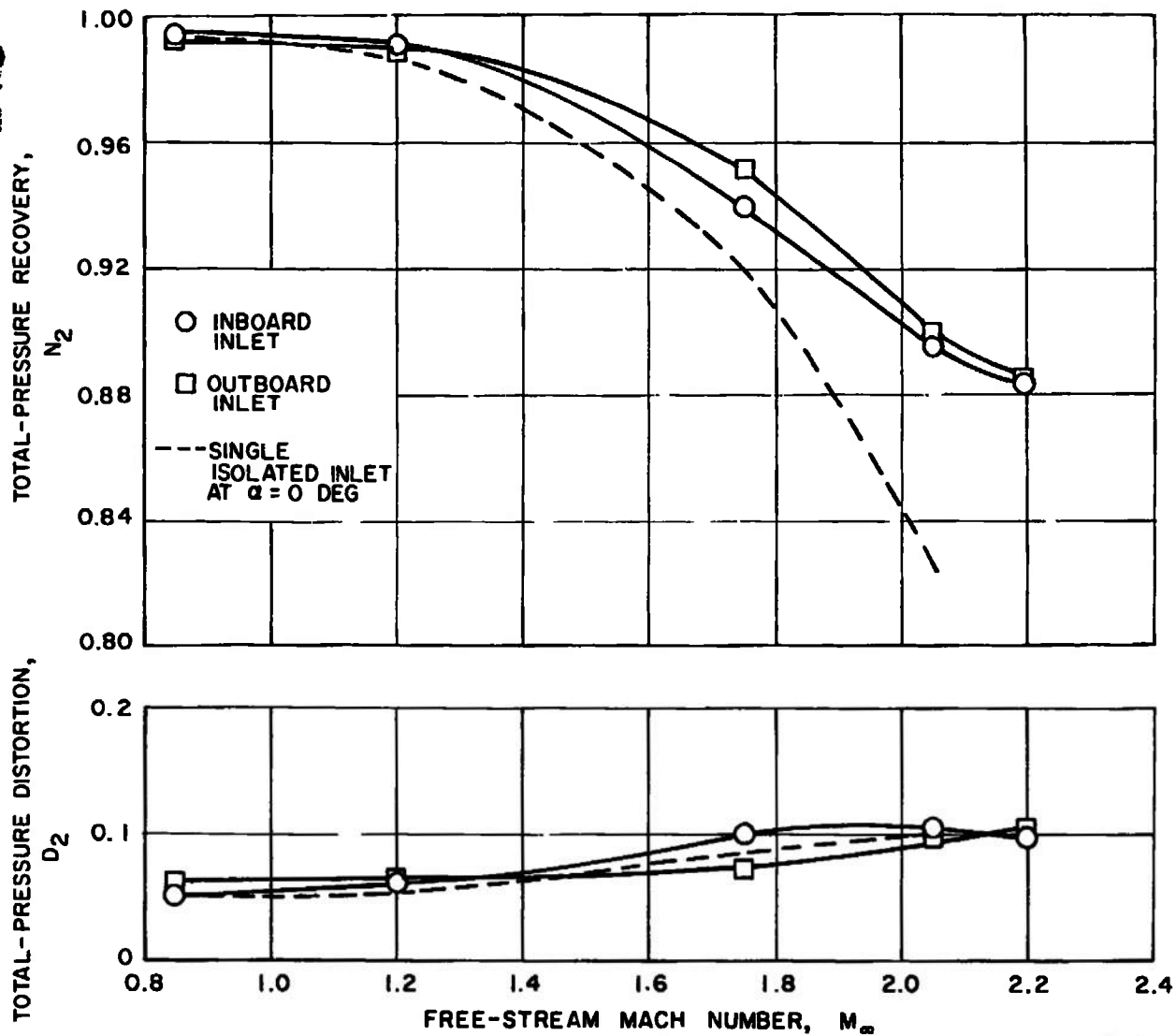
DECLASSIFIED / UNCLASSIFIED

	M_∞	$w\sqrt{B}/82$	$(X/R)_{INB'D}$	$(X/R)_{OUTB'D}$	SPIKE
○	0.85	260	0.60	0.60	I 10
□	1.20	260	0.60	0.60	I 10
◇	1.75	220	1.60	1.63	I 20
△	2.20	180	1.63	1.67	I 27

Fig. 18 Effect of Angle of Sideslip on Inlet Performance; $\alpha = 6.2$ deg

DECLASSIFIED / UNCLASSIFIED

DECLASSIFIED / UNCLASSIFIED

Fig. 19 Optimum Inlet Performance; $\alpha = +5$ deg, $\beta = 0$ deg

SECRET

DECLASSIFIED / UNCLASSIFIED
36

TABLE I
ACCURACY OF MEASUREMENTS

	<u>Uncertainty</u>
Free-stream Mach number, M_∞	
Tunnel 16T	± 0.006
Tunnel 16S	± 0.010
Free-stream total pressure, p_{t_∞} , psf	± 3.000
Compressor-face total-pressure recovery, N_2	± 0.004
Compressor-face total-pressure distortion, D_2	± 0.008
Compressor-face mass-flow ratio, m_2/m_1	± 0.010
Spike bleed mass-flow ratio, m_{sb}/m_1	± 0.001
Simulated full-scale corrected weight flow, $W\sqrt{\theta}/\delta_2$, lb _m /sec	± 2.000
Model total pressure, psf	± 4.000
Model static pressure, psf	± 1.500
Ratio of distance spike tip extends forward of cowl lip to cowl radius, X/R	± 0.003
Free-stream total temperature, T_{t_∞} , °R	± 5.000
Model angle of attack, α , deg	± 0.150
Model angle of sideslip, β , deg	± 0.150

Security Classification

DOCUMENT CONTROL DATA - R & D

(Security classification of title, body of abstract and indexing annotation must be entered when the overall report is classified)

1. ORIGINATING ACTIVITY (Corporate author) Arnold Engineering Development Center ARO, Inc., Operating Contractor Arnold Air Force Station, Tennessee		2a. REPORT SECURITY CLASSIFICATION SECRET	
		2b. GROUP 3	
3. REPORT TITLE WIND TUNNEL INVESTIGATION OF A 1/8-SCALE AMSA AIRCRAFT-INLET MODEL AT TRANSONIC AND SUPERSONIC MACH NUMBERS (U)			
4. DESCRIPTIVE NOTES (Type of report and inclusive dates) Final Report - August 7 through September 9, 1967			
5. AUTHOR(S) (First name, middle initial, last name) Lawrence L. Galigher, ARO, Inc.			
6. REPORT DATE November 1967		7a. TOTAL NO. OF PAGES 46	7b. NO. OF REFS 1
8a. CONTRACT OR GRANT NO. AF40(600)-1200		9a. ORIGINATOR'S REPORT NUMBER(S) AEDC-TR-67-252	
b. PROJECT NO. 139A			
c. Program Element 6340683F		9b. OTHER REPORT NO(S) (Any other numbers that may be assigned this report) N/A	
d.			
10. DISTRIBUTION STATEMENT Subject to special export controls: transmittal to foreign governments or foreign nationals requires approval of ASD (ASZD), Wright-Patterson AFB, Ohio. In addition to security requirements which apply to this document and must be met, each transmittal*			
11. SUPPLEMENTARY NOTES Available in DDC		12. SPONSORING MILITARY ACTIVITY Aeronautical Systems Division, Air Force Systems Command, Wright-Patterson AFB, Ohio	
13. ABSTRACT Test results are presented for a 1/8-scale inlet model of a proposed AMSA air induction system at transonic and supersonic Mach numbers. The effects of spike bleed pattern and inlet orientation are presented. Compressor-face total-pressure recovery and flow distortion data are presented as a function of spike position, compressor-face mass-flow ratio, spike boundary-layer bleed mass-flow ratio, angle of attack, angle of sideslip, and free-stream Mach number. (U)			
<div style="display: flex; justify-content: space-between;"> <div style="width: 20%;"> <p>This document is controlled and released only to foreign nationals (ASZD)</p> </div> <div style="width: 60%; border: 1px solid black; padding: 5px;"> <p>Distribution limited to U. S. Gov't. Agencies only; Test and Evaluation; Nov. 72. Further requests for this document must be referred to Commander, Aeronautical Systems Div., Attn: YHT, Wright-Patterson AFB, Ohio 45433. Per TAB 73-2, 15 January, 1973.</p> </div> <div style="width: 20%;"> <p>controls and release of ASD</p> </div> </div>			
<p>* outside Department of Defense must have prior approval of ASD (ASZD) Wright-Patterson AFB, Ohio.</p>			

14.	KEY WORDS	LINK A		LINK B		LINK C	
		ROLE	WT	ROLE	WT	ROLE	WT
	air induction systems AMSA wind tunnel tests spike bleed patterns air inlets pressure recovery flow distortion mass-flow ratio angle of attack effects angle of sideslip effects Mach number effects transonic flow supersonic flow						
	<i>1. air inlets</i> <i>2. " "</i> <i>3. " "</i> <i>4. Spiked inlets</i> <i>5. " "</i> <i>nozzles</i> <i>1-2.</i>						
	<i>Perform</i> <i>Transonic flow</i> <i>Supersonic</i>						